Classification: Biological Science/Immunology and Inflammation

Evasion of MAIT cell recognition by the African *Salmonella* Typhimurium ST313 pathovar that causes invasive disease.

Lorena Preciado-Llanes[1]*, Anna Aulicino[1], Rocío Canals[2,7], Patrick J. Moynihan[3], Xiaojun Zhu[2], Ndaru Jambo[4], Tonney Nyirenda[4], Innocent Kadwala[4], Ana Sousa Gerós[1], Siân V. Owen[6], Kondwani C. Jambo[4,8], Benjamin Kumwenda[4], Natacha Veerapen[3], Gurdyal S. Besra[3], Melita A. Gordon[4,5], Jay C. D. Hinton[2], Giorgio Napolitani[1], Mariolina Salio[1§*#] & Alison Simmons[1§].

[1]Medical Research Council (MRC) Human Immunology Unit, Medical Research Council Weatherall Institute of Molecular Medicine, University of Oxford, Oxford, OX3 9DS, UK.

[2]Institute of Integrative Biology, University of Liverpool, Liverpool, L69 7ZB, UK.

[3]Institute of Microbiology and Infection, School of Biosciences, University of Birmingham, Edgbaston, Birmingham, B11 2TT, UK.

[4]Malawi-Liverpool-Wellcome Trust Clinical Research Programme, University of Malawi College of Medicine, Blantyre 3, Malawi, Central Africa.

[5]Institute of Infection and Global Health, University of Liverpool, UK

[6]Department of Biomedical Informatics, Harvard Medical School, Boston, Massachusetts, 02115, USA.

[7]Current affiliation: GSK Vaccines Institute for Global Health, 53100, Siena, Italy.

[8]Department of Clinical Sciences, Liverpool School of Tropical Medicine, Liverpool, UK.

[§]Co-senior authors

*Correspondence: mariolina.salio@imm.ox.ac.uk & lorena.preciado-llanes@ndm.ox.ac.uk

[#]Lead contact.

KEY WORDS

Salmonella Typhimurium, sequence type 313, ST313, invasive nontyphoidal *Salmonella*, MR1, MAIT cells, riboflavin, RibB.

SUMMARY

Mucosal-associated invariant T (MAIT) cells are innate T lymphocytes activated by bacteria that produce vitamin B2 metabolites. Mouse models of infection have demonstrated a role for MAIT cells in antimicrobial defence. However, proposed protective roles of MAIT cells in human infections remain unproven and clinical conditions associated with selective absence of MAIT cells have not been identified. We report that typhoidal and non-typhoidal *Salmonella enterica* strains activate MAIT cells. However, *S.* Typhimurium sequence type 313 (ST313) lineage 2 strains, which are responsible for the burden of multidrug-resistant non typhoidal invasive disease in Africa, escape MAIT cell recognition through overexpression of *ribB*. This bacterial gene encodes the 4-dihydroxy-2-butanone-4-phosphate synthase enzyme of the riboflavin biosynthetic pathway. This MAIT cell-specific phenotype did not extend to other innate lymphocytes. We propose that *ribB* overexpression is an evolved trait that facilitates evasion from immune recognition by MAIT cells and contributes to the invasive pathogenesis of *S.* Typhimurium ST313 lineage 2.

STATEMENT OF SIGNIFICANCE

Non-typhoidal *Salmonella* serotypes are a common cause of self-limiting diarrhoeal illnesses in healthy adults. However, recently, a highly invasive multi-drug resistant *Salmonella* Typhimurium sequence type 313 has emerged as a major cause of morbidity and mortality in sub-Saharan Africa, particularly in children and immunosuppressed individuals. In this paper we describe escape from MAIT cell recognition as an additional mechanism of immune evasion of *S.* Typhimurium ST313. As MAIT cells represent an early defence mechanism against pathogens at mucosal surfaces, and their frequency and function are altered in immunosuppressed individuals in sub-Saharan Africa, harnessing their function may offer an important therapeutic strategy to improve mucosal immunity.

\body

INTRODUCTION

The Gram-negative bacterium *Salmonella enterica spp*. comprises many serovars which are closely related phylogenetically but cause very different disease presentations and distinct immune responses in immunocompetent hosts [1], [2]. Infection by the human restricted *Salmonella* typhoidal serovars (*S.* Typhi and *S.* Paratyphi) results in a severe systemic disease called enteric fever. In contrast, nontyphoidal serovars originating from zoonotic reservoirs such as *S.* Typhimurium and *S.* Enteritidis, cause self-limiting diarrhoeal disease in healthy individuals [1]–[3]. Multi-drug resistant *S.* Typhimurium strains of a distinct multilocus sequence type 313 (ST313) recently emerged in sub-Saharan Africa. *S.* Typhimurium ST313 is associated with invasive blood stream infections in immunocompromised individuals and is distinct from the *S.* Typhimurium strains that cause gastroenteritis globally.

Since it was first reported in 2009 [4], the *S.* Typhimurium ST313 clade has become the major cause of invasive nontyphoidal *Salmonella* (iNTS) disease in Africa [5], [6], and comprises two sub-clade lineages [6], termed lineages 1 and 2. Bacteraemia by iNTS causes an estimated 77,500 deaths annually worldwide [7], primarily in Africa, among young children with recent malaria, malarial anaemia or malnutrition and in adults afflicted with HIV, among whom recurrent disease is also common [1], [5], [8]–[11]. *S.* Typhimurium ST313 isolates have rarely been reported outside of Africa [4] and African ST313 blood isolates are genetically distinct from rare diarrhoeal ST313 isolates found in the United Kingdom [12] or Brazil [13]. Genotypic and phenotypic analyses of several clinical isolates of the two well-described ST313 lineages identified signatures of metabolic adaptation and unique enteropathogenesis in animal models, consistent with adaptation to invasive disease in an immunocompromised human population [4], [14], [15].

B and T cell responses can mediate a protective role in mouse models of *Salmonella* infection. B cells provide the first line of defence at mucosal sites to restrain systemic dissemination, while T cells are needed for *Salmonella* clearance [16]–[18]. Cross-reactive and serovar-specific MHC-restricted T cell responses have been well characterised in humans [19]–[24]. *Salmonella* can also induce activation of non-MHC-restricted T cells, specifically $\gamma\delta$ T cells, invariant Natural Killer T cells (iNKT) and Mucosal-associated invariant T (MAIT) cells [25]–[27], although their protective role remains undetermined.

MR1-restricted MAIT cells comprise a highly conserved class of semi invariant T cells, bridging innate and adaptive immunity [28]. The MHC class I-like molecule MR1, bound to derivatives of vitamin B2 intermediates, activates MAIT cells [29]. This process can drive antibacterial activity, *in vitro* and *in vivo*, and correlates with the presence of the vitamin B2 biosynthetic pathway in several commensal and pathogenic bacteria and fungal species (reviewed in [30]). Similar to iNKT and $\gamma\delta$ T cells, MAIT can be activated by cytokines (IL-12, IL-18, type I IFN) independently of their TCR engagement [31]. The ability of MAIT cells to recognise *S.* Typhimurium-infected targets [32] prompted the identification, within bacterial supernatants, of the potent MAIT cell agonists (lumazine and pyrimidines), derivatives of the vitamin B2 intermediate 5-A-RU [29], [33]. Following intranasal infection with *S.* Typhimurium, murine MAIT cells become activated and accumulate in the lungs [26]. Human challenge studies with typhoidal serovars (*S.* Typhi and *S.* Paratyphi A) also demonstrated sustained MAIT cell activation and proliferation at peak of infection [34], [35].

While many commensal and pathogenic bacteria possess the riboflavin biosynthetic pathway, the levels of resulting MAIT stimulation varies [36], [37], perhaps reflecting the influence of microenvironment on bacterial metabolism and antigen availability. The ability of MAIT cells to recognise and respond to several isolates of the same pathogen may also vary depending on metabolic differences between isolates [38].

We hypothesized that MAIT cells contributed to the cellular response to *Salmonella enterica* serovars responsible for invasive disease, and examined the ability of MAIT cells to recognise and respond to different *S. enterica* serovars associated to invasive disease in Africa. Here, we demonstrate that *S.* Typhimurium ST313 lineage 2 isolates escape MAIT cell recognition through overexpression of RibB, a bacterial enzyme of the riboflavin biosynthetic pathway. Our results suggest that MAIT cell immune protection represents an important ‘evolutionary bottleneck’ for the pathogen.

RESULTS

Identification of cellular responses to multiple *Salmonella enterica* subsp *enterica* serovars.

To identify potential differences in the response of innate and adaptive T cells to distinct *Salmonella* pathovars, we focused on two pathovariants of *S.* Typhimurium that are responsible for different types of human disease. *S.* Typhimurium ST313 is associated with invasive disease among immunocompromised individuals in Africa and a representative isolate is D23580 (STM-D23580). *S.* Typhimurium sequence type 19 (ST19) causes non-invasive diarrhoeal infections in immunocompetent individuals globally (a representative isolate is LT2, designated STM-LT2). Peripheral blood mononuclear cells (PBMC) isolated from healthy donors were infected with both *S.* Typhimurium pathovariants, and *S.* Typhi strain Ty2 (ST-Ty2) was used to represent a more distantly related serovar that causes invasive disease in immunocompetent individuals. *Escherichia coli (E. coli)* was included as unrelated control. Upon infection, PBMC were incubated overnight in the presence of brefeldin A to permit intracellular cytokine accumulation. T lymphocytes were stained with a panel of fluorescently labelled antibodies to simultaneously identify different T cell populations (MAIT, $\gamma\delta$, CD4 and CD8), and determine their activation status (CD69) and cytokine production (IFN-γ and TNF-α).

We first defined the heterogeneity of T cell responses to *Salmonella,* by performing an unsupervised clustering analysis on all $CD3^+$ T cells expressing the activation marker CD69 following overnight incubation with the *Salmonella* pathovariants. Dimensionality reduction analysis by *t*-SNE revealed 22 populations of $CD3^+$ $CD69^+$ T cells, some of which differed in frequency according to the infecting *Salmonella* pathogen. Clusters were then annotated and assigned to MAIT (identified as $CD3^+$ $V\alpha7.2^+$ $CD161^{high}$), $\gamma\delta^+$, $CD4^+$ or $CD8^+$ T cell subsets based on the expression of distinct phenotypic markers.

We discovered that a group of clusters of MAIT cells (clusters 6, 15, 18, 21) was under-represented among all $CD69^+$ cells upon infection with STM-D23580, compared with STM-LT2, ST-Ty2 and *E. coli* (Figure 1A). Next, we analysed expression of IFN-γ and TNF-α in $CD69^+$ activated T cells. We determined that the under-represented clusters of $CD69^+$ MAIT cells represented IFN-γ and TNF-α producing MAIT cells (Figure 1B).

MAIT cells were next analysed using Uniform Manifold Approximation and Projection (UMAP), a neighbouring dimensionality reduction technique that preserves embedding and global distances better than t-SNE [39], and clearly defined the trajectory of the distinct subpopulations of *Salmonella*-activated MAIT cells (Figure 1C). STM-LT2 stimulated MAIT cells clustered close to MAIT cells stimulated with ST-Ty2 and *E. coli*, which were characterised by elevated expression of CD69 and the presence of single and double producers of TNF-α and IFN-γ. In contrast, STM-D23580 stimulated MAIT cells clustered closer to unstimulated cells, away from MAIT cells stimulated with ST-Ty2 and *E. coli* (Figure 1D, top left panel). STM-D23580 stimulated MAIT cells expressed low levels of CD69, with only a small TNF-α producing subpopulation and almost no IFN-γ producing cells (Figure 1D).

_S._ Typhimurium ST313 lineage 2 fails to elicit MAIT cell activation in healthy and susceptible individuals.

To validate our unsupervised analysis, we infected PBMC with the different *Salmonella* strains at increasing multiplicity of infection (MOI), and then assessed MAIT cell activation by flow cytometry. Infection by STM-D23580 consistently induced limited MAIT cell responses across a range of MOIs and in every healthy donor tested. In comparison with STM-LT2, ST-Ty2 or *E. coli*, STM-D23580 stimulated MAIT cells significantly expressed less CD69 and produced less IFN-γ and TNF-α (Figure 2A-D). This effect was not dependent on a selective loss of MAIT cells, as STM-D23580 did not have a detrimental effect on MAIT cell viability (SI Appendix, Figure S1A). $\gamma\delta$ T cells, a subset of innate T lymphocytes also present in PBMC, were strongly activated by STM-D23580, indicating that the lack of activation is a phenomenon limited to MAIT cells (Figure 2A, 2C).

In culture, *Salmonella spp.* secrete vitamin B2 intermediates that can bind to MR1 on antigen presenting cells (APCs), to trigger MAIT cell activation [29]. To examine whether STM-D23580 secretes MAIT cell agonists, we collected supernatants from single-colony cultures to stimulate PBMC. Supernatants from STM-LT2 and *E. coli* induced a dose-dependent production of IFN-γ and TNF-α by MAIT cells, whereas STM-D23580 supernatants did not (SI Appendix, Figure S1B).

To validate such findings, we assessed MAIT cell responses to a broader selection of bacterial isolates, including two *S*. Typhi strains (ST-Ty2 and ST-Quailes) and one *S.*

Paratyphi A strain; in addition two differently sourced stocks of STM-D23580 were tested, to ensure that genuine sequence type 313 isolates were being used. At two different MOIs, STM-D23580 elicited the lowest levels of MAIT cell activation of the group (SI Appendix, Figure S1C-S1D). In contrast, γδ T cell responses were comparable across all *Salmonella* pathovars (SI Appendix, Figure S1E-S1F).

We next determined whether the lack of MAIT cell activation was caused by the entire *S.* Typhimurium ST313 clade or was a unique characteristic of ST313 lineage 2 which is currently causing most clinical disease in Africa [14]. STM-D23580 and additional isolates of ST313 lineage 2, were compared with closely-related isolates that were members of ST313 lineage 1 or the UK ST313 group that is associated with gastroenteritis (Figure 2E). To examine MR1-independent MAIT cell activation, we used *Enterococcus faecalis* as a negative control as it lacks the vitamin B2 biosynthetic pathway [29].

Remarkably, only the ST313 strains belonging to lineage 2, such as D23580, D37712 and U60, failed to elicit MAIT cell activation (Figure 2F-2G). All other *Salmonella* ST313 lineages tested (strains U2, U5 and D25248) triggered the same level of MAIT cell responses as *S*. Typhimurium 4/74 (STM-4/74) [40], a sequence type 19 strain that is closely related to STM-LT2 and is associated with non-invasive diarrhoeal infections.

To validate our observations in a relevant population, we performed a series of assays on blood samples obtained from healthy adult residents of Malawi, an endemic area for iNTS infections caused by ST313 strains. We further expanded our investigation into the distinct ST313 clusters by infecting PBMC with four strains from lineage 1, four strains from lineage 2 and four strains from lineage 2.2. Lineage 2.2 comprises multidrug-resistant strains that differ from lineage 2 by 27 single nucleotide polymorphisms [41] and by 4 plasmids [42]. In comparison to the sequence type 19 representative strain STM-4/74, PBMC infected with ST313 lineage 1 strains elicited similar MAIT cell responses, whereas infection with ST313 lineages 2 and 2.2 induced significantly lower levels of MAIT cell responses (Figure 3A and SI Appendix, Fig S2).

Lastly, we extended our findings to a clinically susceptible cohort of HIV-infected adults living in Malawi. In comparison with a cohort of healthy samples from the UK and Malawi, and consistent with previous reports (reviewed in [43]), the overall percentage of MAIT cells was reduced among HIV-infected individuals, particularly in those not

receiving antiretroviral therapy (ART) (Figure 3B). In line with the data obtained with healthy volunteers, MAIT cells from HIV$^+$ adults also failed to produce IFN-γ and TNF-α following *ex vivo* stimulation with STM-D23580, regardless of their ART status (Figure 3C). In contrast, MAIT cells from HIV$^+$ individuals responded strongly to *S.* Typhi and STM-4/74.

These findings suggest that evasion of MAIT cell recognition by sequence type 313 *Salmonella* strains may be a critical factor during the course of natural iNTS disease in endemic populations and in clinically-susceptible groups.

STM-D23580 does not affect MR1-dependent antigen presentation.

To define the molecular mechanisms underlying the lack of MAIT stimulation by STM-D23580, we first investigated whether MAIT cell activation was MR1-dependent. Adding the anti-MR1 blocking antibody 26.5 [44] completely abrogated the MAIT cell activation induced by STM-LT2 and *E. coli*, as well as the minimal activation induced by STM-D23580 (Figure 4A-4B).

We next examined whether STM-D23580 either failed to produce stimulatory MR1 ligands or actively inhibited MAIT cell activation. MAIT cell activation was restored following the addition of the canonical MAIT cell ligand 5-amino-6-D-ribitylaminouracil (5-A-RU) and methylglyoxal (MG) [33] to infected PBMC (Figure 4C-4D), demonstrating that a dominant antagonistic MR1 ligand was not released by STM-D23580. Consistent with these results, a combination of supernatants from overnight cultures of both STM-D23580 and STM-LT2 (added simultaneously or one hour apart) fully restored MAIT cell activation (SI Appendix, Figure S3A-S3B). Likewise, co-infection of PBMC with STM-D23580 plus either STM-LT2, ST-Ty2 or *E. coli* also restored MAIT cell activation to the levels observed with single infections (Figure 4E-4F). Taken together, our data show that STM-D23580 neither interferes nor blocks MAIT cell activation in the presence of stimulatory MR1 ligands.

To exclude the possibility that the lack of MAIT cell activation arose from an insufficient infection of APCs, we exposed Monocyte-derived Dendritic Cells (MoDCs) to fluorescently labelled STM-D23580 or STM-LT2. Live *Salmonella*-containing MoDCs were FACS-sorted and co-cultured with enriched autologous CD3$^+$ T lymphocytes, as described previously [45]. In contrast to STM-LT2 infected MoDCs, STM-D23580

infected MoDCs did not stimulate effector MAIT cells (SI Appendix, Figure S3C). Using an MR1-overexpressing antigen presenting cell line, we found that STM-D23580 supernatants do not cause downregulation of surface MR1 expression, thus excluding this as a possible cause of the lack of MAIT cell activation (SI Appendix, Figure S3D).

Cytokines, such as IL-12, IL-18 and type I IFN, released by APCs upon bacterial or viral infection can also activate MAIT cells in a MR1-independent manner [31]. We confirmed that when MoDCs were co-cultured with purified MAIT cells, equal amounts of bioactive IL-12p70 were secreted upon infection with STM-D23580, STM-LT2 and *E. coli* (SI Appendix, Figure S3E).

Taken together, these observations refuted the hypothesis that lack of MAIT cell activation is caused by an impaired MR1-dependent antigen-presentation following STM-D23580 infection.

STM-D23580 evades MAIT cell recognition by overexpression of RibB.

The observation that STM-D23580 and related ST313 isolates do not interfere with MR1 presentation or cytokine production suggests that these bacteria might not produce the MR1 binding ligands that are generated by other *S.* Typhimurium or *S.* Typhi pathovariants. The major source of natural antigens driving MAIT cell activation derives from by-products of microbial riboflavin synthesis [33]. We depict the *Salmonella* riboflavin biosynthetic pathway in Figure 5A. A comparison of the coding sequences (CDS) of the enzymes involved in the riboflavin biosynthesis pathway found only one nucleotide change (SNP) between the sequence type 19 STM-4/74 and the sequence type 313 STM-D23580 strains. This synonymous coding variant was located in the *ribD* gene (Glu316Glu) [46], suggesting that there were no biochemical differences between the riboflavin biosynthesis pathways of the sequence type 313 and sequence type 19 isolates.

To determine whether the enzymes of the riboflavin pathway of the sequence type 19 STM-4/74 and sequence type 313 STM-D23580 strains were expressed at different levels, we investigated the transcriptomic and proteomic data from our recent comparative analysis [46]. Strains STM-4/74 and STM-D23580 are closely-related, sharing 92% of coding genes [46]. Differential gene expression analysis of the *rib* genes at the transcriptomic level identified significant up-regulation of *ribB* ($\geq$2 fold-change, FDR $\leq$0.001) in STM-D23580 in four out of the five experimental conditions

(Figure 5B). We then examined data from a quantitative proteomic approach which showed that RibB protein levels were up-regulated in STM-D23580 compared to STM-4/74, during growth in rich medium at early stationary phase (ESP) (Figure 5C).

We searched for a molecular explanation for the high levels of *ribB* expression in STM-D23580 compared to STM-4/74. In STM-D23580, *ribB* and its 5' untranslated region (5'UTR) are transcribed as a single transcript that is initiated from a single gene promoter which we identified previously [46]. By analogy with the genetic mechanism identified for over-expression of the PgtE virulence factor in STM-D23580 [47] we searched for nucleotide polymorphisms that distinguished the *ribB* regions of the two strains. There were no differences between the promoter sequences of the *ribB* genes or the 5' UTR of the strains STM-D23580 and STM-4/74.

To determine whether the MAIT cell activation phenotype was linked to the overexpression of the RibB enzyme (4-dihydroxy-2-butanone 4-phosphate synthase), we created a derivative of STM-4/74 that expressed high levels of RibB. Since deletions in the riboflavin biosynthetic pathway genes are lethal without high dose riboflavin supplementation [33][48] and *ribB* is essential for *Salmonella in vivo* virulence [49], we used a gene cloning approach to overexpress the *ribB* gene of STM-D23580 in STM-4/74 from a recombinant plasmid (STM-4/74 RibB^{++}). The expression of high levels of the RibB enzyme by STM-4/74 ablated MAIT cell activation induced by wild-type STM-4/74. Infection with STM-4/74 RibB^{++} induced low levels of cytokine production and CD69 expression by MAIT cells, recapitulating the phenotype of STM-D23580 (Figure 5D-5E). Importantly, $\gamma\delta$ T cells responded equally to both STM-4/74 wild type and STM-4/74 RibB^{++} (SI Appendix, Figure S4).

We next evaluated the bacterial growth rate, as well as the infection efficiency of the STM-4/74 RibB^{++} bacterial strain. Mid-log phase curves demonstrated no significant differences in the growth rate between STM-4/74 wild type, STM-4/74 RibB^{++} and other related strains (SI Appendix, Figure S5A). Human monocyte-derived dendritic cells and human monocyte-derived macrophages were infected *in vitro,* and the number of intracellular bacterial colony-forming units (cfu) was measured as a readout of internalisation. In both cell types tested, the number of recovered intracellular STM-4/74 RibB^{++} was comparable to the number obtained from other *Salmonella* strains (SI Appendix, Figure S5B). These data exclude the possibility that the lack of MAIT activation by STM-4/74 RibB^{++} reflects slow growth or poor bacterial internalisation into antigen-presenting cells.

MAIT activator ligands such as 5-OP-RU (5- (2-oxopropylideneamino)-6-D-ribitylaminouracil) or 5-OE-RU (5- (2-oxoethylideneamino)-6-D-ribitylaminouracil), products of the riboflavin pathway, cannot be measured due to their unstable nature [33]. Therefore, to investigate whether overexpression of RibB altered the balance of downstream products from the riboflavin pathway, we measured the amount of riboflavin, flavin mononucleotide (FMN) and flavin adenine dinucleotide (FAD) by HPLC. Following growth to early stationary phase, intracellular samples and culture supernatants from STM-4/74 and STM-4/74 RibB^{++} contained larger amounts of riboflavin than the sequence type 313 strains STM-D23580 and STM-D37712 (Figure 6A-6B). The STM-4/74 RibB^{++} supernatant with the highest level of riboflavin also contained the largest amount of FMN, compared with STM-4/74, STM-D23580 and STM-D37712 (Figure 6C).

Overall, the data show that the RibB over-producing strain (4/74 RibB^{++}) produced the highest level of extracellular riboflavin and FMN, whereas had the lowest level of intracellular FMN. In contrast, the STM-4/74 wild-type strain had the largest intracellular amount of FMN, compared with 4/74 RibB^{++} and both of the sequence type 313 strains (Figure 6D). While intracellular FAD levels were similar between STM-4/74, STM-D23580 and STM-D37712, STM-4/74 RibB^{++} contained the lowest level of intracellular FAD (Figure 6E). We conclude that the lowest levels of intracellular FMN was found in the STM-D23580, STM-D37712 and STM-4/74 RibB^{++} strains that overexpress the RibB enzyme.

Reduced MAIT cell antibacterial activity against *S.* Typhimurium ST313 lineage 2 infected macrophages.

To test the role of MAIT cells in clearing *Salmonella* infections, we developed an *in vitro* assay where human monocyte-derived macrophages were infected with the different *Salmonella* strains, either in presence or absence of purified MAIT cells. As observed with PBMC, we measured less IFN-γ in supernatants from co-cultures of purified MAIT cells and macrophages infected with STM-4/74 RibB^{++} and sequence type 313 lineage 2 strains, as compared to the control sequence type 19 strains (SI Appendix, Figure S6A).

In these experiments, the number of intracellular cfu recovered from infected macrophages was used as a surrogate of bactericidal activity induced by MAIT cells.

In the majority of the biological replicates and in comparison with macrophages alone, we observed a modest reduction of cfu numbers (25% or less) when MAIT cells and sequence type 313 lineage 2 infected macrophages were put in co-culture (SI Appendix, Figure S6B). In contrast, almost all biological replicates infected with sequence type 19 *Salmonella* had a reduction of more than 25% in the number of cfu when MAIT cells were added to the infected macrophages (SI Appendix, Figure S6B). No differences in bactericidal activity were observed between STM-4/74 RibB^{++} and STM-4/74. While macrophages pre-treated with IFN-γ acquired bactericidal activity against all *Salmonella* isolates (SI Appendix, Figure S6C), MAIT cell anti-microbial activity in these *in vitro* co-cultures was not directly correlated to the amount of IFN-γ found in supernatants (SI Appendix, Figure S6D).

DISCUSSION

Here we investigated the ability of MAIT cells to recognise and respond to diverse invasive *Salmonella enterica* serovars. We found that MAIT cells isolated from the blood of healthy individuals were not activated by exposure to invasive disease-associated *S.* Typhimurium sequence type 313 (ST313) lineage 2 strains. Our data demonstrated how *S.* Typhimurium ST313 lineage 2 evades MAIT cell recognition by overexpressing *ribB*, a bacterial gene encoding the RibB enzyme involved in the riboflavin pathway. Our results lead us to propose that this RibB-mediated mechanism provides an evolutionary advantage that allows invasive *S.* Typhimurium ST313 lineage 2 bacteria to escape cell immune responses by overexpressing a single riboflavin bacterial gene.

MR1-restricted MAIT cells are highly abundant in the gut mucosa [50], where they reach their final maturation upon recognition of vitamin B2 metabolites derived from gut commensals presented by MR1 expressing mucosal B cells [50]. MAIT cells show antimicrobial activity *in vivo* and *in vitro* [51], [52] through MR1 dependent and independent interactions. Microorganisms must express the riboflavin biosynthesis pathway to be able to activate MAIT cells [29], [53]. Mutations in key enzymes of the riboflavin biosynthetic pathway in both Gram positive and negative bacteria can abrogate MAIT cell activation [33], [54]. Different bacteria that possess the riboflavin biosynthetic pathway induce varying levels of MAIT stimulation [36], [37], possibly through the influences of the microenvironment on bacterial metabolism and antigen availability, or the known short half-life of the potent MAIT cell antigens, 5-OP-RU and 5-OE-RU [55]. The ability of MAIT cells to recognise and respond to several isolates of the same pathogen may also vary to reflect bacterial metabolic differences. For example, riboflavin metabolism variation among clinical isolates of *Streptococcus pneumoniae* produces different measurable levels of riboflavin and FMN that correlate with differential activation of MAIT cells [38].

Salmonella spp. possess an active riboflavin biosynthetic pathway, which generates MAIT cell agonists [29], [33]. MAIT cells recognise and kill *S.* Typhimurium-infected targets *in vitro* [32], and activated MAIT cells accumulate in murine lungs following intranasal infection with *S.* Typhimurium [26]. However, bacterial lung clearance was independent of MAIT cells in this infection model, possibly due to the non-physiological route of infection. While some mouse models of infection with *Salmonella* sequence type 313 strains have been published [14], [56] , these models present limited utility as

mice have very low frequencies and absolute numbers of MAIT cells compared with humans [28]. Human studies demonstrated sustained MAIT cell activation and proliferation at the peak of infection with *S.* Typhi and *S.* Paratyphi [34], [35]. Among immunocompetent humans, the clinical outcomes of infection by *Salmonella enterica* spp. depend on the infecting serovar. Human-restricted typhoidal serovars, such as *S.* Typhi induce the most severe form of systemic disease, typhoid fever; while the broad-host *S.* Typhimurium sequence type 19 causes self-limiting gastroenteritis. The recently documented multidrug resistant *S.* Typhimurium ST313 clade causes the majority of iNTS cases among immunocompromised adults and malnourished young children living in sub-Saharan Africa.

Several bacterial factors have been reported to enhance invasiveness of *S.* Typhimurium ST313, suggesting a multifactorial adaptation of this African lineage to a systemic lifestyle. These include interference with the complement cascade [47], interference with DC function [45], reduced inflammasome activation [57], dissemination through $CD11b^+$ migratory DC [58] among others.

Here we found that *S.* Typhi, *S.* Paratyphi A and most *S.* Typhimurium pathovars potently elicited *ex vivo* MR1-dependent MAIT cell activation, but all tested isolates from the invasive *S.* Typhimurium ST313 lineage 2 barely induced cytokine secretion or CD69 upregulation. This suboptimal activation was restricted to MAIT cells, as $\gamma\delta$ cell activation was comparable across all isolates tested. We excluded differences in infection efficiency, MR1 expression, co-stimulatory cytokines (IL-12), the genetic sequence of the riboflavin encoding enzymes of *S.* Typhimurium and the presence of dominant inhibitory ligands as potential mechanisms for these results. Following comparative proteomic and transcriptomic analyses, we discovered that invasive *S.* Typhimurium ST313 lineage 2 pathovars escape MAIT cell recognition by overexpressing *ribB*, a bacterial gene encoding the riboflavin biosynthetic enzyme RibB. By overexpressing this single riboflavin gene in a sequence type 19 *S.* Typhimurium strain, we revealed that up-regulation of this single riboflavin gene was sufficient to abrogate MAIT cell responses.

Transcriptional control of the bacterial *ribB* gene is controlled by a conserved FMN riboswitch, which is located in the 5′ untranslated region (5’ UTR) of *ribB* [59], and is negatively regulated by FMN and other flavins at the transcriptional and translational levels in *E. coli* [60]. The SroG small RNA (sRNA) is derived from the *ribB* 5’ leader sequence, although the function of this sRNA remains unknown [61]. In addition to the

riboswitch-mediated regulation, RibB expression is induced by growth in a low pH environment [62]. In STM-D23580, both *sroG* and *ribB* are transcribed as a single transcript that is initiated from a single gene promoter which we identified previously [46].

While the precise molecular mechanism responsible for *ribB* overexpression remains to be established, a single noncoding nucleotide polymorphism in the promoter of the *pgtE* gene of the ST313 lineage 2 strain STM-D23580 is known to be responsible for high expression of the outer membrane PgtE virulence factor, which promotes bacterial survival and dissemination during mammalian infection [47]. The lack of nucleotide differences between the promoter sequences of the *ribB* genes or the riboswitch of the two strains suggests that the high level of expression of *ribB* in STM-D23580 is caused by a novel and uncharacterised regulatory mechanism.

It has been proposed that genomic changes in ST313 isolates that confer altered metabolism and increased anaerobic metabolic capacity are linked to adaptation of the extra-intestinal niche [14]. Riboflavin and its derivatives are important cofactors for flavoproteins involved in cellular redox metabolism and several biochemical pathways, proposed to be essential for the metabolic adaptation of the ST313 clade. Riboflavin promotes intracellular microbial survival and virulence during *in vivo* infection with *Histoplasma capsulatum* and *Brucella abortus* [63], [64]. In addition, accumulation of riboflavin is a candidate virulence factor in *Pseudogymnoascus destructans* skin infection [65].

The metabolomic measurements of the end-products of the riboflavin pathway showed a correlation between lower levels of intracellular FMN and increased expression of RibB. Because FMN is a negative regulator of *ribB* gene expression [60], we speculate that the lower levels of intracellular FMN observed in the ST313 strains D23580 and D37712 are linked to the high levels of expression of RibB in these African *S.* Typhimurium strains.

Overall, our findings suggest that MAIT cells play a crucial role in defence against invasive *Salmonella* disease in humans and that evasion from MAIT cell recognition is a critical mechanism for the invasiveness of *S*. Typhimurium ST313 lineage 2 isolates, including those belonging to the lineage 2.2 cluster [41]. We propose that differences in MAIT cells activation may associate to distinct diseases caused by closely related microorganisms. The increased susceptibility of immunocompromised patients to the

513 *S*. Typhimurium ST313 lineage 2 strains suggests that MAIT cells might play a
514 particularly relevant role in the context of waning $CD4^+$ T cell mediated protective
515 adaptive immunity, where protection relies mostly on the innate immune response. For
516 example, following HIV co-infection and/or malnutrition, among individuals suffering
517 from recurrent gut infections secondary to intestinal barrier dysfunction [66], [67],
518 microbiota dysbiosis [68], [69] and multiple innate and adaptive immune defects [70].
519 Our findings may be of major relevance during the initial phase of infection, in the gut,
520 where it is expected that resident immune cells such as MAIT cells should prevent
521 systemic infection by encountering and responding rapidly to bacterial signals. We
522 propose that the ability of MAIT cells to target gastrointestinal pathogens represents a
523 key immunological evolutionary bottleneck that has been effectively countered by
524 *Salmonella,* resulting in the current epidemic of invasive disease in Africa.
525
526
527

METHODS

Bacterial strains and preparation of stocks.

This study included representative strains of *Salmonella enterica* serovar Typhimurium, from both the sequence type 19 and the sequence type 313. *S.* Typhi and *S.* Paratyphi A serovars were utilised as comparative Typhoidal invasive strains, while *Escherichia coli* (DH5α) was used as unrelated bacterial control. Supplementary Table 1 lists bacterial strains used in this study.

Overnight bacterial cultures from a single colony origin were used to inoculate LB Lennox broth (Sigma) supplemented with sucrose (Sigma) at a final concentration of 10%. Inoculated cultures were incubated at 37ºC under constant shaking for approximately 3 hours, until reaching mid logarithmic phase. Bacterial aliquots were prepared and immediately frozen at -80ºC for long-term storage. Bacterial viability of frozen aliquots was monitored periodically in order to maintain experimental reproducibility. The number of viable colony forming units (cfu) was determined with the Miles and Misra method, by plating 10-fold dilutions of the bacterial suspension onto LB Lennox agar (Sigma). On the day of the experiment, a single aliquot was thawed, washed twice with PBS and re-suspended in RPMI 1640 media to obtain the desired multiplicity of infection (MOI).

In the case of bacterial supernatants, these were taken from late exponential phase cultures, grown from a single colony following 18 hours incubation under constant shaking. Supernatants were filter sterilised before using.

Construction of *S.* Typhimurium 4/74 pP_L-*ribB*

To construct pP_L-*ribB*, the *ribB* gene was amplified from genomic DNA of *S.* Typhimurium 4/74 using primers *ribB*_FW and *ribB*_RV. The PCR product was used for a linear amplification reaction with plasmid pJV300 (pP_L) using Phusion DNA polymerase (New England Biolabs), and the resulting product was digested with DpnI. The plasmid was transformed into *E. coli* TOP10 and selected on LB plates supplemented with 100 µg/mL ampicillin. Plasmid presence was confirmed by PCR and DNA sequencing using oligonucleotides pPL_Seq_FW and pPL_Seq_RV. The pP_L-*ribB* plasmid was subsequently purified and transformed into *S.* Typhimurium 4/74. Supplementary Table 2 lists plasmids and oligonucleotides used in this study.

Isolation of human cells from peripheral blood from healthy volunteers in the UK.

Leukocyte Reduction System cones were obtained from the UK National Blood Centre with informed consent following local ethical guidelines (NHSTB account T293). Blood was diluted in PBS and separated by gradient centrifugation using Lymphoprep™ (AxisShield). Peripheral Blood Mononuclear Cells (PBMC) were collected from the interface, washed with PBS, resuspended in complete medium and counted. Complete medium used throughout was RPMI 1640 (Sigma), supplemented with 10% heat-inactivated FCS (Sigma), 2 mM L-glutamine, 1% nonessential amino acids and 1% sodium pyruvate (all from Gibco).

Isolation of PBMC from healthy and HIV-infected volunteers in Malawi.

Blood samples were obtained at Queen Elizabeth Central Hospital (Blantyre, Malawi) following local ethical guidelines (P09/17/2284). Adults presenting for HIV testing at the voluntary testing clinic, the HIV outpatient clinic, and the medical inpatient wards at the Queen Elizabeth Central Hospital were recruited. Based on the use of antiretroviral therapy, these patients were classified as ART naïve (without) or ART treated (with). Upon appropriate consent and medical authorisation, a blood sample was collected and PBMC were isolated and used in *ex vivo* infection assays, as described below.

***Ex vivo* infection assays with PBMC**

PBMC were seeded in 96 well plates round bottom (5 to 8 $x10^5$ cells per well) and infected with the different *Salmonella* strains from frozen mid-log phase stocks, at the indicated MOI. Upon 80 minutes incubation at 37°C, 100 μg/mL gentamicin (Lonza) was added to kill extracellular bacteria. 200 μg/mL of gentamicin was required for the experiments carried out in Malawi using ST313 strains from lineages 1, 2 and 2.2.
At 180 minutes post-infection, 5ng/mL brefeldin A (BioLegend) solution was added to every well in order to achieve accumulation of intracellular cytokines. Samples were incubated overnight at 37°C for no more than 15 hours.
For MR1 blocking experiments, infection was performed in the presence of 30 μg/mL MR1 blocking antibody 26.5 [44] or mouse IgG2a isotype control (ATCC). The MAIT agonists 5-Amino-6-D-ribitylaminouracil (5-A-RU) was synthesised as described [71] and 1 μg/mL was combined to 50 μM methylglyoxal (MG, Sigma).

Assessment of cytokine production and MAIT cell activation by flow cytometry.

Following incubation in the presence of brefeldin A, cells were harvested, washed and stained with a viability dye (live/dead Zombie Aqua, BioLegend) for 20 minutes.

Fixation was performed for 30 minutes at 4°C using the Foxp3 Fixation/Permeabilization buffers (eBioscience). Fixed cells were permeabilised and stained with an antibody cocktail for 40 minutes at room temperature, washed and stored protected from light at 4°C in PBS with 0.5% bovine serum albumin (FACS buffer) until acquisition. The following antibodies were used for extracellular and intracellular staining as 2 different panels: anti-CD3 Alexa700 (clone UCHT1; BioLegend), anti-CD3 PerCp Cy5.5 (clone UCHT1; BioLegend), anti-CD4 APCef780 (clone RPA-T4; eBioscience), anti-CD4 Alexa700 (clone RPA-T4; BioLegend), anti-CD8 BV785 (clone RPA-T8; BioLegend), anti-TCR γ/δ APC (clone B1; BioLegend), anti-CD161 BV605 (clone HP-3G10; BioLegend), anti-CD161 BV421 (clone HP-3G10; BioLegend), anti-Vα7.2 PE (clone 3C10; BioLegend), anti-Vα7.2 PE-Cy7 (clone 3C10; BioLegend), anti-CD69 FITC (clone FN50; BioLegend), anti TNF-α PECy7 (clone Mab11; BioLegend), anti TNF-α APC (clone Mab11; BioLegend), anti-IFN-γ FITC (clone 4S.B3; BioLegend) and anti-IFN-γ PE Dazzle (clone 4S.B3; BioLegend). Samples from the UK were acquired on a FortessaX20 (BD), whilst samples from the case-control study in Malawi were acquired on a LSR Fortessa cytometer (BD). All data was analysed with the same gating strategy on FlowJo (v.10.6.1).

Unsupervised analysis of flow cytometry data.

Two dimensionality reduction methods based on a neighbouring graph approach were implemented, t-Distributed Stochastic Neighbour Embedding (t-SNE) [72] and Uniform Manifold Approximation and Projection (UMAP) [73]. t-SNE algorithm was performed on the Cytofkit platform [74] using up to 5,000 cells from each sample. UMAP was run as a plugin on FlowJo (v.10.4.1) using 15 nearest neighbours, a minimum distance of 0.5 and Euclidean distance for selected parameters. Files with .fcs extension from related experimental conditions were concatenated before UMAP analysis.

Co-culture of *Salmonella* infected monocyte-derived dendritic cells and purified T cells.

Monocyte-derived dendritic cells (MoDCs) were obtained from PBMC by enrichment of $CD14^+$ monocytes using magnetic beads (Miltenyi). Differentiation was achieved with recombinant human GM-CSF (40 ng/mL) and human IL-4 (40ng/mL), both from PeproTech. After 5 days, MoDCs were infected with violet-labelled (CellTracker™, Life Technologies) *Salmonella* strains, either STM-D23580 or STM-LT2 at an MOI of 10, as reported elsewhere [45].

635 At six hours post-infection, *Salmonella*-containing MoDCs were FACS sorted as single
636 cells. Sorted MoDCs were co-cultured with magnetically enriched (Miltenyi) $CD3^+$ T
637 cells obtained from the same donor, at a ratio of 1 MoDC per 6 T cells. Following 12
638 hours incubation in the presence of brefeldin A, T cells were harvested and stained for
639 intracellular cytokines as described above.
640
641 **Co-culture of *Salmonella* infected MoDCs and expanded MAIT cells.**
642 Human MoDCs were obtained as described above. Human MAIT cells were isolated
643 by sorting CD2 MACS-enriched (Miltenyi) leukocytes with CD161 and Vα7.2
644 antibodies (BioLegend). MAIT cells were grown for around 6 weeks in complete RPMI
645 media supplemented with IL-2, as described elsewhere [71].
646 40,000 MoDCs and 20,000 MAIT cells (2:1 ratio) were seeded in 96 well plates flat
647 bottom and were infected at MOI of 3.5. After 80 minutes, 100 µg/mL gentamicin was
648 added and supernatants were harvested following 26 hours incubation. IL-12 p70 was
649 measured by ELISA (R&D systems) in triplicates and following manufacturer's
650 instructions.
651
652 **Co-culture of *Salmonella* infected monocyte-derived macrophages and**
653 **expanded MAIT cells.**
654 Monocytes were obtained from leukocyte reduction system cones by enrichment of
655 $CD14^+$ cells using magnetic beads (Miltenyi), according to manufacturer's protocol.
656 Monocytes were seeded in 24-well plates (450,000 - 500,000 cells/well) and
657 differentiated into macrophages using recombinant human M-CSF at 100 ng/mL
658 (PeproTech). After 6 days of incubation at 37ºC and 5% CO_2, the adherent
659 macrophages were carefully washed to remove M-CSF containing-media and fresh
660 antibiotic-free medium was added. Next, macrophages were infected with the different
661 *Salmonella* strains at a MOI of 15. After 30 minutes post-infection, cells were washed
662 and incubated for further 30 minutes with 100 µg/mL of gentamicin-containing medium
663 to kill any remaining extracellular bacteria. At 1 hour post-infection, macrophages were
664 washed again and MAIT cells were added (ratio 1 MAIT cell per 5 macrophages) into
665 the respective wells. From this point and onwards, media contained gentamicin at 30
666 µg/mL as maintenance dose. Cells were incubated until completing 6 hours post-
667 infection before being washed twice with PBS and lysed with 2% saponin. The number
668 of intracellular viable bacterial cfu was determined with the Miles and Misra method as
669 described above. IFN-γ in the supernatants was measured with a commercial ELISA
670 (BD-Pharmingen), as per manufacturer instructions.

MR1 over-expressing cell line

THP-1 cells were transduced with an MR1 encoding lentivirus [34]. MR1 overexpressing cells were seeded in 96 well plates flat bottom and incubated overnight in the presence of 50 µL of supernatants from bacterial cultures at late exponential phase, or in the presence of 5-A-RU as positive control. Cells were harvested, washed and stained for surface expression of MR1 (clone 26.5; BioLegend) by flow cytometry. Expression of MHC-I (clone G46-2.6, BD Biosciences) was also monitored as unrelated control.

Transcriptomic and proteomic analyses of riboflavin enzymes.

RNA-seq and proteomic data for genes involved in the riboflavin biosynthetic pathway were extracted from a recent work [46]. Briefly, a differential expression comparative analysis between strains STM-D23580 and STM-4/74 was performed at the transcriptomic level in five *in vitro* infection-relevant conditions: ESP (early stationary phase), anaerobic growth, NonSPI2 (SPI2-non-inducing PCN), InSPI2 (SPI2-inducing PCN) and inside murine RAW264.7 macrophages (ATCC TIB-71). Specific details about growing bacteria in these conditions had been previously described [40], [75]. For a comparative proteomic analysis, bacteria were grown to ESP in the LB rich medium.

The RNA-seq-based comparative approach between STM-D23580 and STM-4/74 was based on Voom/Limma analysis from three different biological replicates for each strain. A detailed pipeline for the analysis can be found in Canals *et.al.* [46].

Proteomic data for strains STM-D23580 and STM-4/74 were obtained using an LC-MS/MS (Q Exactive Orbitrap, 4h reversed phase C18 gradient) platform. Samples included six biological replicates for each strain. Label-free quantification and differential expression analyses between the two strains were performed using the Progenesis QI software (Nonlinear Dynamics) [46].

Measurement of riboflavin, FMN and FAD in supernatants and pellets of bacterial cultures.

Bacterial pellets and supernatants from early stationary phase cultures (OD_{600}=~2), were prepared in triplicate and frozen at -80 ^{o}C. For extraction of cellular flavins, pellets were resuspended in 100 µL of 100 mM ammonium formate, 100 mM formic acid, 25% (v/v) methanol and heated at 80 ^{o}C for 10 min. Insoluble material was removed by centrifugation. For analysis 5 µL of this material or the culture supernatants was

separated by HPLC on a Dionex UPLC system with a Kinetex C18 column (Phenomenex; 1.7 um, 150 x 2.1 mm). Separation was achieved at 45 ºC and 0.2 mL/min isocractically using 20 mM potassium phosphate buffer (pH 2.5) with 25% methanol (v/v) over 8 min followed by a 1 min wash step in 100% methanol. Flavins were detected with fluorescence (450 nm excitation, 520 nm emission) and peaks were quantified by comparison to known standards. For normalisation the total pmol of flavin for each culture was divided by the measured OD600 of the cultures to give a final pmol/OD_{600} value.

Statistical analysis

Statistical analyses were performed using GraphPad-Prism8 (GraphPad Software; San Diego, United States). Differences among groups were determined by paired one-way, two-way ANOVA or Kruskal-Wallis as appropriate. Post-hoc corrections were applied, Dunnett's or Dunn's for comparisons to a control data set and Bonferroni's, Tukey's or Sidak's for comparisons of selected pairs tests, as appropriate. A *p*-value <0.05 was considered statistically significant (**p* <0.05, ***p* <0.01, ****p* <0.001 and *****p* <0.0001).

Data Availability

All data has been made available in the manuscript.

FIGURE LEGENDS

Figure 1. Identification of cellular responses to multiple *Salmonella enterica* subsp *enterica* serovars.

PBMC were left unstimulated or were infected at MOI of 5 with STM-D23580, STM-LT2, ST-Ty2 or *E. coli*. Intracellular staining was performed to detect CD69 expression and cytokine production (TNF-α and IFN-γ), as correlates of T cell activation. **(A)** *t*-SNE plots on gated CD69$^+$ CD3$^+$ T cells infected with STM-D23580, STM-LT2, ST-Ty2 or *E. coli*. Four CD3$^+$ T cell populations (CD4$^+$, CD8$^+$, $\gamma\delta^+$ and MAIT) were annotated based on the expression of distinct phenotypic markers. CD4, CD8, TCR$\gamma\delta$, Vα7.2$^+$, CD161, IFN-γ and TNF-α were the parameters included for *t*-SNE analysis. Plots correspond to one representative donor. **(B)** *t*-SNE plots as in (A) showing relative expression of TNF-α and IFN-γ on CD69$^+$ CD3$^+$ T cells. **(C)** UMAP analysis on concatenated CD3$^+$ Vα7.2$^+$ CD161$^+$ MAIT cells from the same donor as in (A) and (B). Calculated UMAPs are shown for each experimental condition. CD69, IFN-γ and TNF-α were the parameters included for analysis. **(D)** Top left panel showing UMAP as an overlay of concatenated MAIT cell populations from (C): unstimulated in light grey, STM-D23580 in blue, STM-LT2 in green, ST-Ty2 in red and *E. coli* in dark grey. Top right and bottom panels: UMAPs showing expression of CD69, TNF-α and IFN-γ in pink. **(A-D)** Data from one donor representative of four biological replicates.

Figure 2. *S.* Typhimurium ST313 lineage 2 fails to elicit MAIT cell activation.

PBMC were left unstimulated (U) or were infected with a variety of *Salmonella* strains at the indicated MOI. *E coli* was included as positive control and *E. faecalis* as negative control. **(A)** Production of TNF-α and IFN-γ by MAIT and $\gamma\delta^+$ T cells was detected by intracellular staining. Representative flow cytometry plots from one volunteer are shown. **(B)** Percentage of TNF-α and/or IFN-γ producing MAIT cells when stimulated at increasing MOI, from 0.5 to 20 bacteria per cell. Data represented as mean $\pm$ SEM, two-way ANOVA + Dunnet's, *n*=4. **(C)** CD69 staining profile of stimulated MAIT and $\gamma\delta^+$ T cells. Representative histograms from one volunteer are shown. **(D)** CD69 expression on MAIT cells when stimulated as in (B). Data represented as geometric mean $\pm$ SEM, two-way ANOVA + Dunnet's, *n*=4. **(E)** Phylogenetic relationships between strains used in these experiments (red) within the context of *Salmonella enterica* phylogeny. **(F)** Percentage of TNF-α and/or IFN-γ producing MAIT cells, treated with bacterial strains at MOI of 2.5 and 5. Data represented as mean $\pm$ SEM, two-way ANOVA + Dunnet's, *n*=4. **(G)** Levels of CD69 expression on MAIT cells

765 treated as in (E). Data represented as geometric mean ± SEM, two-way ANOVA +
766 Dunnet's, *n*=4.
767
768 **Figure 3. Characterisation of MAIT cell responses to *Salmonella spp*. in relevant**
769 **and susceptible cohorts of individuals.**
770 **(A)** PBMC were isolated from ten healthy individuals living in Malawi. Cells were
771 infected at MOI of 7 with various strains from sequence type 313 (ST313) lineages 1,
772 2 and 2.2 or with the sequence type 19 (ST19) reference strain STM-4/74. Each dot
773 represents the average of TNF-α and/or IFN-γ producing MAIT cells per individual
774 upon stimulation with 4 strains from each lineage (see Figure S2). Median ± IQR,
775 Friedman + Dunn's, *n*=10 for each group. **(B)** Percentage of MAIT cells ($CD3^+$ $V\alpha7.2^+$
776 $CD161^+$) in PBMC isolated from healthy (*n*=12) and HIV-infected individuals living in
777 Malawi, with (*n*=6) or without ART (*n*=6). Data represented as percentage of live $CD3^+$
778 T cells, median with IQR, Kruskal-Wallis + Dunn's. **(C)** PBMC isolated from HIV^+
779 patients with or without ART were infected at MOI of 7 with either STM-D23580, STM-
780 4/74, STy-H58 or *E. coli*. PMA/ionomycin was used as positive control. Data
781 represented as percentage of TNF-α and/or IFN-γ producing MAIT cells, mean ± SEM,
782 one-way ANOVA + Dunnet's, *n*=6 for each group.
783
784 **Figure 4. STM-D23580 does not affect MR1-dependent antigen presentation.**
785 **(A)** PBMC were infected (at MOI 2.5 and 7.5) with STM-D23580 (blue), STM-LT2
786 (green) or *E. coli* (grey), and incubated in the presence of anti-MR1 blocking antibody
787 or the equivalent isotype control. Data are represented as percentage of TNF-α and/or
788 IFN-γ producing MAIT cells, box-and-whisker plot, two-way ANOVA + Dunnet's, *n*=4.
789 **(B)** Representative example of cytokine production by stimulated MAIT cells treated
790 as in (A). **(C- D)** PBMC were left unstimulated or were infected (at MOI 2.5 and 5) with
791 either STM-D23580 or STM-LT2, in the presence (pink bars) or absence (grey bars)
792 of the MR1 ligands 5-A-RU and MG. Percentage of cytokine producing MAIT cells and
793 their CD69 expression are shown. Data represented as mean and geometric mean ±
794 SEM, two-way ANOVA + Bonferroni's, *n*=4. **(E)** PBMC were infected with D23580 at
795 MOI of 2.5, alone or in combination with STM-LT2 (green), ST-Ty2 (orange) or *E. coli*
796 (grey), at two different MOI (2.5 and 5). Data represented as percentage of TNF-α
797 and/or IFN-γ producing MAIT cells, mean ± SEM, one-way ANOVA + Sidak's, *n*=5. **(F)**
798 Representative example of cytokine production by stimulated MAIT cells treated as in
799 (E).
800

Figure 5. STM-D23580 evades MAIT cell recognition by overexpression of *ribB*. (**A**) Schematic representation of *Salmonella*'s riboflavin pathway, adapted from Soudais *et al*. [54]. **(B)** The relative transcriptional expression levels of the *ribABDEFH* genes were derived from our published RNA-seq data set [46]. The gene expression values from STM-D23580 and STM-4/74 were determined in five infection-relevant conditions: ESP (early stationary phase), anaerobic growth, NonSPI2 (SPI2-non-inducing PCN), InSPI2 (SPI2-inducing PCN), and macrophage (intra-RAW264.7 murine macrophage environment). Values indicate fold-change (FC) and false discovery rate (FDR), calculated from a Voom/Limma analysis (using Degust) for the RNA-seq data comparison of STM-D23580 versus STM-4/74. Data represent three biological replicates. PCN = phosphate carbon nitrogen minimal medium. **(C)** The relative expression levels of the RibABDEFH proteins were derived from our published proteomic data set for the ESP condition [46]. The heat map shows differential expression analysis following comparison between STM-D23580 and STM-4/74. Results from LC-MS/MS were analysed using the Progenesis QI software (Nonlinear Dynamics) for label-free quantification analysis. Each sample represents six biological replicates. Data represented in panels **B** and **C** were extracted from Canals *et.al.* [46]. **(D)** PBMC were infected at two different MOI (2 and 5) with STM-D23580 (blue), STM-4/74 (green) or STM-4/74 RibB^{++} (pink). Data represented as percentage of TNF-α and/or IFN-γ producing MAIT cells, mean $\pm$ SEM, two-way ANOVA + Tukey's, n=6. **(E)** CD69 staining profile of stimulated MAIT cells treated as in (D). Representative histograms from one volunteer are shown, MFI=Median Fluorescence Intensity.

Figure 6. STM-4/74 RibB^{++} has the lowest intracellular levels of FMN, a negative regulator of *ribB* gene expression.

Supernatants from early stationary phase and bacterial pellets were harvested and analysed by HLPC using riboflavin, FMN and FAD standards. Data is reported in pmol and has been normalised to the absorbance (OD_{600}) from each culture. **(A)** Riboflavin levels in supernatants. **(B)** Intracellular riboflavin levels. **(C)** FMN levels in supernatants. **(D)** Intracellular FMN levels. **(D)** Intracellular FAD levels. Measurements were obtained from 3 biological replicates, mean $\pm$ SEM, one-way ANOVA + Dunnet's.

ACKNOWLEDGMENTS

This work was supported by an NIHR Research Professorship and a Wellcome Trust Investigator Award (A.S.), the UK Medical Research Council through the MRC Human Immunology Unit (G.N., M.S and A.S.) and Celgene (A.A.). Part of this work was supported by a Wellcome Trust Senior Investigator award (to JCDH) (Grant 106914/Z/15/Z). PM was supported by a BBSRC David Phillips Fellowship (Grant BB/S010122/1). We acknowledge support of the Oxford NIHR Biomedical Research Centre. The views expressed are those of the authors and not necessarily those of the NHS, the NIHR or the Department of Health. We thank Dr. Ted Hansen for the gift of the anti-MR1 26.5 Ab. We acknowledge the contribution of Paul Sopp and Craig Waugh in the flow cytometry facility at the Weatherall Institute of Molecular Medicine for cell sorting experiments. We acknowledge the assistance of Priyanka Patel, Joyce Macheso, Anstead Kankwatira, and the Malawi-Liverpool-Wellcome Trust clinical team.

AUTHOR CONTRIBUTIONS

Conceptualization L.P-L. M.S. and A.S.; Writing- Review & Editing, L.P-L., M.S., R.C., J.C.D.H., G.N., M.A.G. and A.S.; Methodology, L.P-L., M.S., R.C., A.A., P.M. and G.N.; Investigation, L.P-L., A.A., R.C., P.M., X.Z., N.J., I.K. and A.S.G; Visualization, L.P-L., M.S., R.C. and P.M; Resources J.C.D.H., S.V.O., N.V., G.S.B., K.J., B.K., M.A.G. and T.N.; Supervision and funding, M.S and A.S.

CONFLICT OF INTEREST

Rocío Canals was employed by the University of Liverpool at the time of the study and is now an employee of the GSK group of companies. The other authors declare no conflict of interest.

REFERENCES

[1] N. A. Feasey, G. Dougan, R. A. Kingsley, R. S. Heyderman, and M. A. Gordon, "Invasive non-typhoidal salmonella disease: an emerging and neglected tropical disease in Africa.," *Lancet (London, England)*, vol. 379, no. 9835, pp. 2489–2499, Jun. 2012.

[2] A. M. Keestra-Gounder, R. M. Tsolis, and A. J. Bäumler, "Now you see me, now you don't: the interaction of Salmonella with innate immune receptors.," *Nat. Rev. Microbiol.*, vol. 13, no. 4, pp. 206–16, Apr. 2015.

[3] M. Achtman *et al.*, "Multilocus sequence typing as a replacement for serotyping in Salmonella enterica.," *PLoS Pathog.*, vol. 8, no. 6, p. e1002776, 2012.

[4] R. A. Kingsley *et al.*, "Epidemic multiple drug resistant Salmonella Typhimurium causing invasive disease in sub-Saharan Africa have a distinct genotype.," *Genome Res.*, vol. 19, no. 12, pp. 2279–87, Dec. 2009.

[5] E. A. Reddy, A. V Shaw, and J. A. Crump, "Community-acquired bloodstream infections in Africa: a systematic review and meta-analysis.," *Lancet. Infect. Dis.*, vol. 10, no. 6, pp. 417–32, Jun. 2010.

[6] C. K. Okoro *et al.*, "Intracontinental spread of human invasive Salmonella Typhimurium pathovariants in sub-Saharan Africa," *Nat. Genet.*, vol. 44, no. 11, pp. 1215–1221, Nov. 2012.

[7] J. D. Stanaway *et al.*, "The global burden of non-typhoidal salmonella invasive disease: a systematic analysis for the Global Burden of Disease Study 2017," *Lancet Infect. Dis.*, vol. 19, no. 12, pp. 1312–1324, Dec. 2019.

[8] J. A. Berkley *et al.*, "HIV infection, malnutrition, and invasive bacterial infection among children with severe malaria.," *Clin. Infect. Dis.*, vol. 49, no. 3, pp. 336–43, Aug. 2009.

[9] H. M. Biggs *et al.*, "Invasive Salmonella infections in areas of high and low malaria transmission intensity in Tanzania.," *Clin. Infect. Dis.*, vol. 58, no. 5, pp. 638–47, Mar. 2014.

[10] M. A. Gordon, "Salmonella infections in immunocompromised adults," *J. Infect.*, vol. 56, no. 6, pp. 413–422, Jun. 2008.

[11] M. A. Gordon *et al.*, "Non-typhoidal salmonella bacteraemia among HIV-infected Malawian adults: high mortality and frequent recrudescence.," *AIDS*, vol. 16, no. 12, pp. 1633–41, Aug. 2002.

[12] P. M. Ashton *et al.*, "Public health surveillance in the UK revolutionises our understanding of the invasive Salmonella Typhimurium epidemic in Africa.," *Genome Med.*, vol. 9, no. 1, p. 92, 2017.

[13] F. Almeida *et al.*, "Multilocus sequence typing of Salmonella Typhimurium reveals the presence of the highly invasive ST313 in Brazil.," *Infect. Genet. Evol.*, vol. 51, pp. 41–44, 2017.

[14] C. K. Okoro *et al.*, "Signatures of adaptation in human invasive Salmonella Typhimurium ST313 populations from sub-Saharan Africa.," *PLoS Negl. Trop. Dis.*, vol. 9, no. 3, p. e0003611, Mar. 2015.

[15] B. N. Parsons *et al.*, "Invasive non-typhoidal Salmonella Typhimurium ST313 are not host-restricted and have an invasive phenotype in experimentally infected chickens.," *PLoS Negl. Trop. Dis.*, vol. 7, no. 10, p. e2487, 2013.

[16] a J. Griffin and S. J. McSorley, "Development of protective immunity to Salmonella, a mucosal pathogen with a systemic agenda.," *Mucosal Immunol.*, vol. 4, no. 4, pp. 371–382, 2011.

[17] J. Hess, C. Ladel, D. Miko, and S. H. Kaufmann, "Salmonella Typhimurium aroA- infection in gene-targeted immunodeficient mice: major role of CD4+ TCR-alpha beta cells and IFN-gamma in bacterial clearance independent of intracellular location.," *J. Immunol.*, vol. 156, no. 9, pp. 3321–6, May 1996.

[18] S.-J. Lee, S. Dunmire, and S. J. McSorley, “MHC class-I-restricted CD8 T cells play a protective role during primary Salmonella infection.,” *Immunol. Lett.*, vol. 148, no. 2, pp. 138–43, Dec. 2012.
[19] G. Napolitani *et al.*, “Clonal analysis of Salmonella-specific effector T cells reveals serovar-specific and cross-reactive T cell responses.,” *Nat. Immunol.*, vol. 19, no. 7, pp. 742–754, Jul. 2018.
[20] C. J. Reynolds *et al.*, “The serodominant secreted effector protein of Salmonella, SseB, is a strong CD4 antigen containing an immunodominant epitope presented by diverse HLA class II alleles.,” *Immunology*, vol. 143, no. 3, pp. 438–46, Nov. 2014.
[21] R. Wahid, S. Fresnay, M. M. Levine, and M. B. Sztein, “Cross-reactive multifunctional CD4+ T cell responses against Salmonella enterica serovars Typhi, Paratyphi A and Paratyphi B in humans following immunization with live oral typhoid vaccine Ty21a.,” *Clin. Immunol.*, vol. 173, pp. 87–95, Dec. 2016.
[22] A. Sheikh *et al.*, “Interferon-γ and proliferation responses to Salmonella enterica Serotype Typhi proteins in patients with S. Typhi Bacteremia in Dhaka, Bangladesh.,” *PLoS Negl. Trop. Dis.*, vol. 5, no. 6, p. e1193, Jun. 2011.
[23] S. H. Pennington *et al.*, “Oral Typhoid Vaccination With Live-Attenuated Salmonella Typhi Strain Ty21a Generates Ty21a-Responsive and Heterologous Influenza Virus–Responsive CD4 + and CD8 + T Cells at the Human Intestinal Mucosa,” *J. Infect. Dis.*, vol. 213, no. 11, pp. 1809–1819, Jun. 2016.
[24] T. S. Nyirenda *et al.*, “Sequential acquisition of T cells and antibodies to nontyphoidal Salmonella in Malawian children.,” *J. Infect. Dis.*, vol. 210, no. 1, pp. 56–64, Jul. 2014.
[25] M. Brigl, L. Bry, S. C. Kent, J. E. Gumperz, and M. B. Brenner, “Mechanism of CD1d-restricted natural killer T cell activation during microbial infection.,” *Nat. Immunol.*, vol. 4, no. 12, pp. 1230–7, Dec. 2003.
[26] Z. Chen *et al.*, “Mucosal-associated invariant T-cell activation and accumulation after in vivo infection depends on microbial riboflavin synthesis and co-stimulatory signals.,” *Mucosal Immunol.*, vol. 10, no. 1, pp. 58–68, 2017.
[27] A. Davies *et al.*, “Infection-induced expansion of a MHC Class Ib-dependent intestinal intraepithelial gammadelta T cell subset.,” *J. Immunol.*, vol. 172, no. 11, pp. 6828–37, Jun. 2004.
[28] O. Lantz and F. Legoux, “MAIT cells: an historical and evolutionary perspective,” *Immunol. Cell Biol.*, vol. 96, no. 6, pp. 564–572, Jul. 2018.
[29] L. Kjer-Nielsen *et al.*, “MR1 presents microbial vitamin B metabolites to MAIT cells,” *Nature*, vol. 491, pp. 717–723, 2012.
[30] D. I. Godfrey, H.-F. Koay, J. McCluskey, and N. A. Gherardin, “The biology and functional importance of MAIT cells.,” *Nat. Immunol.*, Aug. 2019.
[31] J. E. Ussher *et al.*, “CD161++ CD8+ T cells, including the MAIT cell subset, are specifically activated by IL-12+IL-18 in a TCR-independent manner,” *Eur J Immunol*, vol. 44, pp. 195–203, 2014.
[32] R. Reantragoon *et al.*, “Structural insight into MR1-mediated recognition of the mucosal associated invariant T cell receptor,” *J Exp Med*, vol. 209, no. 4, pp. 761–774, 2012.
[33] A. J. Corbett *et al.*, “T-cell activation by transitory neo-antigens derived from distinct microbial pathways,” *Nature*, vol. 509, pp. 361–365, 2014.
[34] L. J. Howson *et al.*, “MAIT cell clonal expansion and TCR repertoire shaping in human volunteers challenged with Salmonella Paratyphi A,” *Nat. Commun.*, vol. 9, no. 1, p. 253, 2018.
[35] R. Salerno-Goncalves *et al.*, “Challenge of Humans with Wild-type Salmonella enterica Serovar Typhi Elicits Changes in the Activation and Homing

Characteristics of Mucosal-Associated Invariant T Cells.," *Front. Immunol.*, vol. 8, p. 398, 2017.

[36] M. Schmaler *et al.*, "Modulation of bacterial metabolism by the microenvironment controls MAIT cell stimulation," *Mucosal Immunol*, vol. 11, pp. 1060–1070, 2018.

[37] C. Tastan *et al.*, "Tuning of human MAIT cell activation by commensal bacteria species and MR1-dependent T-cell presentation," *Mucosal Immunol.*, vol. 11, no. 6, pp. 1591–1605, Nov. 2018.

[38] N. Hartmann *et al.*, "Riboflavin Metabolism Variation among Clinical Isolates of Streptococcus pneumoniae Results in Differential Activation of Mucosal-associated Invariant T Cells," *Am J Respir Cell Mol Biol*, vol. 58, pp. 767–776, 2018.

[39] E. Becht *et al.*, "Dimensionality reduction for visualizing single-cell data using UMAP," *Nat. Biotechnol.*, vol. 37, no. 1, pp. 38–44, Dec. 2018.

[40] C. Kröger *et al.*, "An infection-relevant transcriptomic compendium for Salmonella enterica Serovar Typhimurium.," *Cell Host Microbe*, vol. 14, no. 6, pp. 683–95, Dec. 2013.

[41] C. L. Msefula *et al.*, "Genotypic homogeneity of multidrug resistant S. Typhimurium infecting distinct adult and childhood susceptibility groups in Blantyre, Malawi.," *PLoS One*, vol. 7, no. 7, p. e42085, 2012.

[42] B. Kumwenda *et al.*, "The distinct genomic and transcriptomic signature of a novel sub-lineage 2.2 of invasive non-typhoidal Salmonella Typhimurium ST313," *Manuscr. Prep.*

[43] J. A. Juno, C. Phetsouphanh, P. Klenerman, and S. J. Kent, "Perturbation of mucosal-associated invariant T cells and iNKT cells in HIV infection.," *Curr. Opin. HIV AIDS*, vol. 14, no. 2, pp. 77–84, Mar. 2019.

[44] S. Huang *et al.*, "Evidence for MR1 antigen presentation to mucosal-associated invariant T cells," *J Biol Chem*, vol. 280, no. 22, pp. 21183–21193, 2005.

[45] A. Aulicino *et al.*, "Invasive Salmonella exploits divergent immune evasion strategies in infected and bystander dendritic cell subsets.," *Nat. Commun.*, vol. 9, no. 1, p. 4883, 2018.

[46] R. Canals *et al.*, "Adding function to the genome of African Salmonella Typhimurium ST313 strain D23580.," *PLoS Biol.*, vol. 17, no. 1, p. e3000059, Jan. 2019.

[47] D. L. Hammarlöf *et al.*, "Role of a single noncoding nucleotide in the evolution of an epidemic African clade of Salmonella.," *Proc. Natl. Acad. Sci. U. S. A.*, vol. 115, no. 11, pp. E2614–E2623, 2018.

[48] E. H. Battley, "Escherichia Coli and Salmonella Typhimurium. Cellular and Molecular Biology, Volume 1; Volume 2 . Frederick C. Neidhardt , John L. Ingraham , Boris Magasanik , K. Brooks Low , Moselio Schaechter , H. Edwin Umbarger," *Q. Rev. Biol.*, vol. 63, no. 4, pp. 463–464, Dec. 1988.

[49] C. Rollenhagen and D. Bumann, "Salmonella enterica highly expressed genes are disease specific.," *Infect. Immun.*, vol. 74, no. 3, pp. 1649–60, Mar. 2006.

[50] E. Treiner *et al.*, "Selection of evolutionarily conserved mucosal-associated invariant T cells by MR1," *Nature*, vol. 422, pp. 164–169, 2003.

[51] E. W. Meermeier, M. J. Harriff, E. Karamooz, and D. M. Lewinsohn, "MAIT cells and microbial immunity.," *Immunol. Cell Biol.*, vol. 96, no. 6, pp. 607–617, Jul. 2018.

[52] M. Salou, K. Franciszkiewicz, and O. Lantz, "MAIT cells in infectious diseases.," *Curr. Opin. Immunol.*, vol. 48, pp. 7–14, Oct. 2017.

[53] L. Le Bourhis *et al.*, "Antimicrobial activity of mucosal-associated invariant T cells," *Nat Immunol*, vol. 11, pp. 701–708, 2010.

[54] C. Soudais *et al.*, "In Vitro and In Vivo Analysis of the Gram-Negative Bacteria-Derived Riboflavin Precursor Derivatives Activating Mouse MAIT Cells," *J*

Immunol, vol. 194, pp. 4641–4649, 2015.
[55] J. Y. Mak *et al.*, "Stabilizing short-lived Schiff base derivatives of 5-aminouracils that activate mucosal-associated invariant T cells," *Nat Commun*, vol. 8, p. 14599, 2017.
[56] J. Yang *et al.*, "Characterization of the Invasive, Multidrug Resistant Non-typhoidal Salmonella Strain D23580 in a Murine Model of Infection," *PLoS Negl. Trop. Dis.*, vol. 9, no. 6, p. e0003839, Jun. 2015.
[57] S. Carden, C. Okoro, G. Dougan, and D. Monack, "Non-typhoidal Salmonella Typhimurium ST313 isolates that cause bacteremia in humans stimulate less inflammasome activation than ST19 isolates associated with gastroenteritis.," *Pathog. Dis.*, vol. 73, no. 4, Jun. 2015.
[58] S. E. Carden *et al.*, "Pseudogenization of the Secreted Effector Gene ssel Confers Rapid Systemic Dissemination of S. Typhimurium ST313 within Migratory Dendritic Cells.," *Cell Host Microbe*, vol. 21, no. 2, pp. 182–194, Feb. 2017.
[59] M. S. Gelfand, A. A. Mironov, J. Jomantas, Y. I. Kozlov, and D. A. Perumov, "A conserved RNA structure element involved in the regulation of bacterial riboflavin synthesis genes.," *Trends Genet.*, vol. 15, no. 11, pp. 439–42, Nov. 1999.
[60] D. Pedrolli, S. Langer, B. Hobl, J. Schwarz, M. Hashimoto, and M. Mack, "The ribB FMN riboswitch from Escherichia coli operates at the transcriptional and translational level and regulates riboflavin biosynthesis.," *FEBS J.*, vol. 282, no. 16, pp. 3230–42, Aug. 2015.
[61] J. Vogel *et al.*, "RNomics in Escherichia coli detects new sRNA species and indicates parallel transcriptional output in bacteria.," *Nucleic Acids Res.*, vol. 31, no. 22, pp. 6435–43, Nov. 2003.
[62] L. M. Stancik, D. M. Stancik, B. Schmidt, D. M. Barnhart, Y. N. Yoncheva, and J. L. Slonczewski, "pH-dependent expression of periplasmic proteins and amino acid catabolism in Escherichia coli.," *J. Bacteriol.*, vol. 184, no. 15, pp. 4246–58, Aug. 2002.
[63] H. R. Bonomi *et al.*, "An atypical riboflavin pathway is essential for Brucella abortus virulence.," *PLoS One*, vol. 5, no. 2, p. e9435, Feb. 2010.
[64] A. L. Garfoot, O. Zemska, and C. A. Rappleye, "Histoplasma capsulatum depends on de novo vitamin biosynthesis for intraphagosomal proliferation.," *Infect. Immun.*, vol. 82, no. 1, pp. 393–404, Jan. 2014.
[65] M. Flieger *et al.*, "Vitamin B2 as a virulence factor in Pseudogymnoascus destructans skin infection.," *Sci. Rep.*, vol. 6, p. 33200, 2016.
[66] J. K. Roche, A. Cabel, J. Sevilleja, J. Nataro, and R. L. Guerrant, "Enteroaggregative Escherichia coli (EAEC) impairs growth while malnutrition worsens EAEC infection: a novel murine model of the infection malnutrition cycle.," *J. Infect. Dis.*, vol. 202, no. 4, pp. 506–14, Aug. 2010.
[67] J. Yu *et al.*, "Environmental Enteric Dysfunction Includes a Broad Spectrum of Inflammatory Responses and Epithelial Repair Processes.," *Cell. Mol. Gastroenterol. Hepatol.*, vol. 2, no. 2, pp. 158-174.e1, Feb. 2016.
[68] S. Subramanian *et al.*, "Persistent gut microbiota immaturity in malnourished Bangladeshi children.," *Nature*, vol. 510, no. 7505, pp. 417–21, Jun. 2014.
[69] M. I. Smith *et al.*, "Gut microbiomes of Malawian twin pairs discordant for kwashiorkor.," *Science*, vol. 339, no. 6119, pp. 548–54, Feb. 2013.
[70] C. D. Bourke, J. A. Berkley, and A. J. Prendergast, "Immune Dysfunction as a Cause and Consequence of Malnutrition.," *Trends Immunol.*, vol. 37, no. 6, pp. 386–398, Jun. 2016.
[71] M. Salio *et al.*, "Activation of Human Mucosal-Associated Invariant T Cells Induces CD40L-Dependent Maturation of Monocyte-Derived and Primary Dendritic Cells," *J Immunol*, vol. 199, pp. 2631–2638, 2017.
[72] L. J. P. van der Maaten and G. E. Hinton, "Visualizing high-dimensional data

using t-SNE," *J. Mach. Learn. Res.*, vol. 9, pp. 2579–2605, 2008.
[73] L. McInnes, J. Healy, N. Saul, and L. Großberger, "UMAP: Uniform Manifold Approximation and Projection," *J. Open Source Softw.*, vol. 3, no. 29, p. 861, Sep. 2018.
[74] H. Chen, M. C. Lau, M. T. Wong, E. W. Newell, M. Poidinger, and J. Chen, "Cytofkit: A Bioconductor Package for an Integrated Mass Cytometry Data Analysis Pipeline.," *PLoS Comput. Biol.*, vol. 12, no. 9, p. e1005112, Sep. 2016.
[75] S. Srikumar *et al.*, "RNA-seq Brings New Insights to the Intra-Macrophage Transcriptome of Salmonella Typhimurium.," *PLoS Pathog.*, vol. 11, no. 11, p. e1005262, 2015.

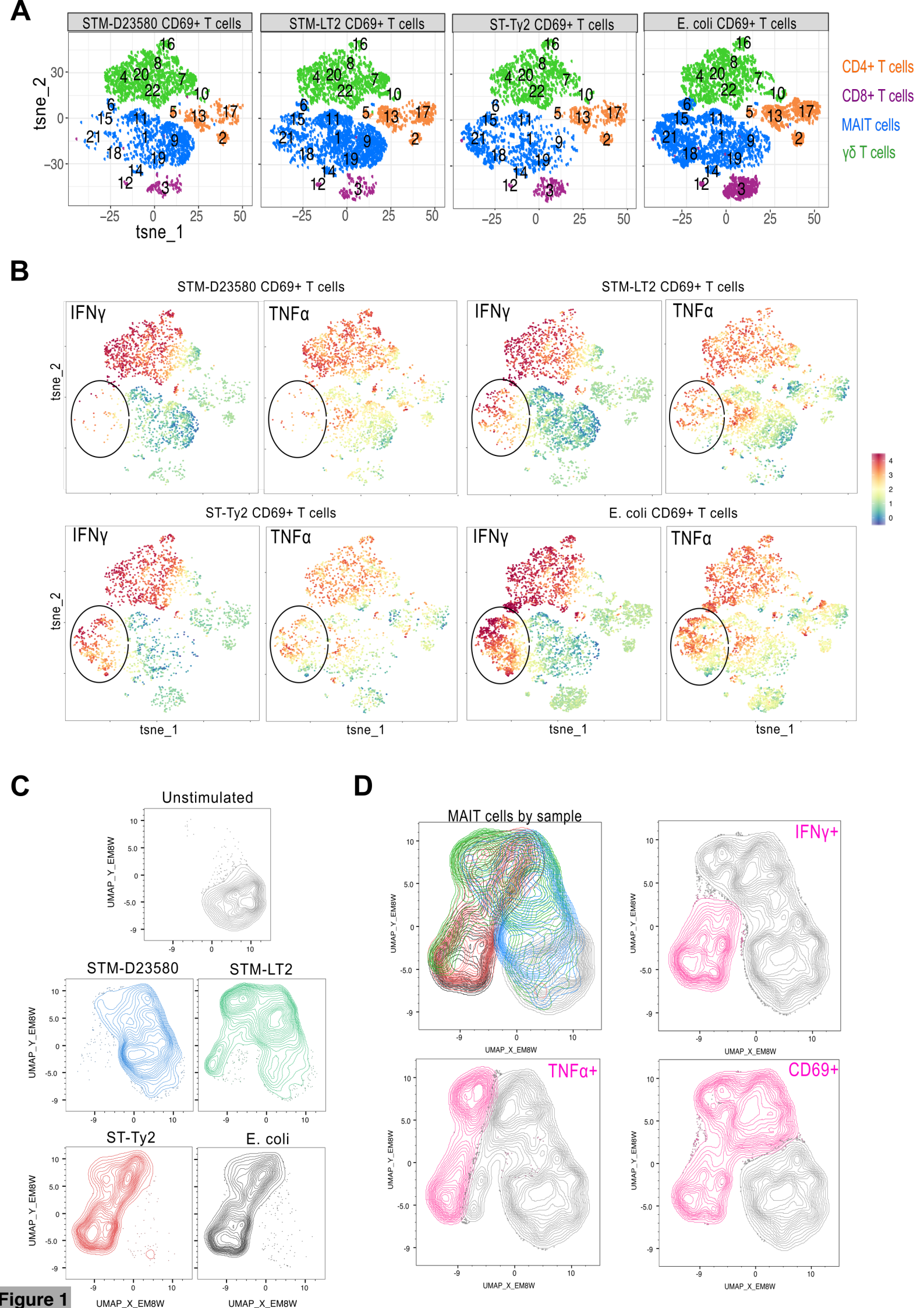
A
STM-D23580 CD69+ T cells
STM-LT2 CD69+ T cells
ST-Ty2 CD69+ T cells
E. coli CD69+ T cells
tsne_2
tsne_1
CD4+ T cells
CD8+ T cells
MAIT cells
γδ T cells
B
STM-D23580 CD69+ T cells
STM-LT2 CD69+ T cells
ST-Ty2 CD69+ T cells
E. coli CD69+ T cells
IFNγ
TNFα
tsne_2
tsne_1
C
Unstimulated
STM-D23580
STM-LT2
ST-Ty2
E. coli
UMAP_Y_EM8W
UMAP_X_EM8W
D
MAIT cells by sample
IFNγ+
TNFα+
CD69+
UMAP_Y_EM8W
UMAP_X_EM8W

Figure 1

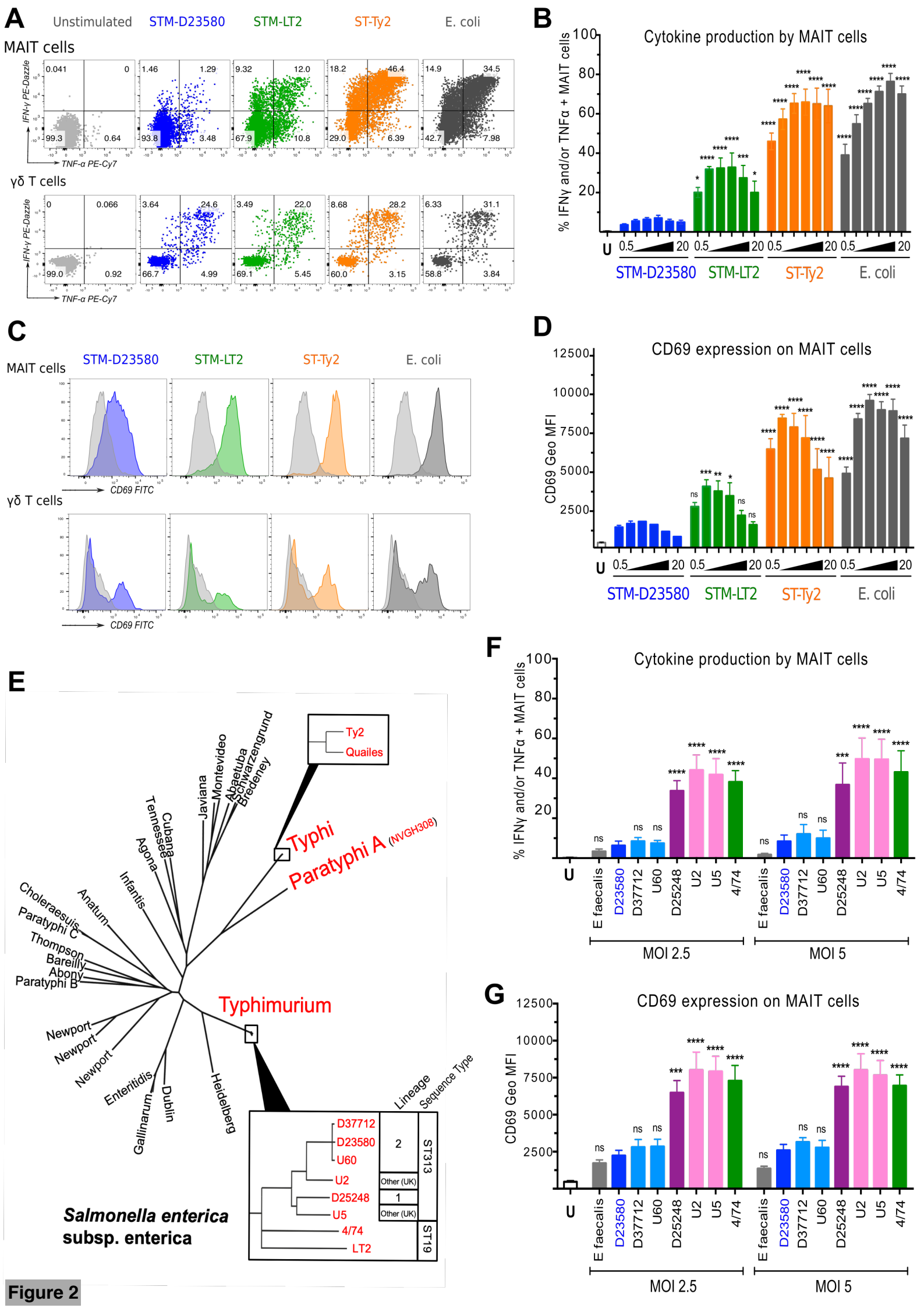
A
Unstimulated
STM-D23580
STM-LT2
ST-Ty2
E. coli
MAIT cells
IFN-γ PE-Dazzle
TNF-α PE-Cy7
0.041
0
99.3
0.64
1.46
1.29
93.8
3.48
9.32
12.0
67.9
10.8
18.2
46.4
29.0
6.39
14.9
34.5
42.7
7.98
γδ T cells
0
0.066
99.0
0.92
3.64
24.6
66.7
4.99
3.49
22.0
69.1
5.45
8.68
28.2
60.0
3.15
6.33
31.1
58.8
3.84
B
Cytokine production by MAIT cells
% IFNγ and/or TNFα + MAIT cells
U
0.5
20
STM-D23580
STM-LT2
ST-Ty2
E. coli
C
MAIT cells
STM-D23580
STM-LT2
ST-Ty2
E. coli
CD69 FITC
γδ T cells
D
CD69 expression on MAIT cells
CD69 Geo MFI
E
Ty2
Quailes
Typhi
Paratyphi A (NVGH308)
Typhimurium
Javiana
Montevideo
Abaetuba
Schwarzengrund
Bredeney
Cubana
Tennessee
Agona
Infantis
Anatum
Choleraesuis
Paratyphi C
Thompson
Bareilly
Abony
Paratyphi B
Newport
Newport
Newport
Enteritidis
Gallinarum
Dublin
Heidelberg
Lineage
Sequence Type
D37712
D23580
U60
U2
D25248
U5
4/74
LT2
2
Other (UK)
1
Other (UK)
ST313
ST19
Salmonella enterica
subsp. enterica
F
Cytokine production by MAIT cells
% IFNγ and/or TNFα + MAIT cells
U
E faecalis
D23580
D37712
U60
D25248
U2
U5
4/74
MOI 2.5
MOI 5
G
CD69 expression on MAIT cells
CD69 Geo MFI

Figure 2

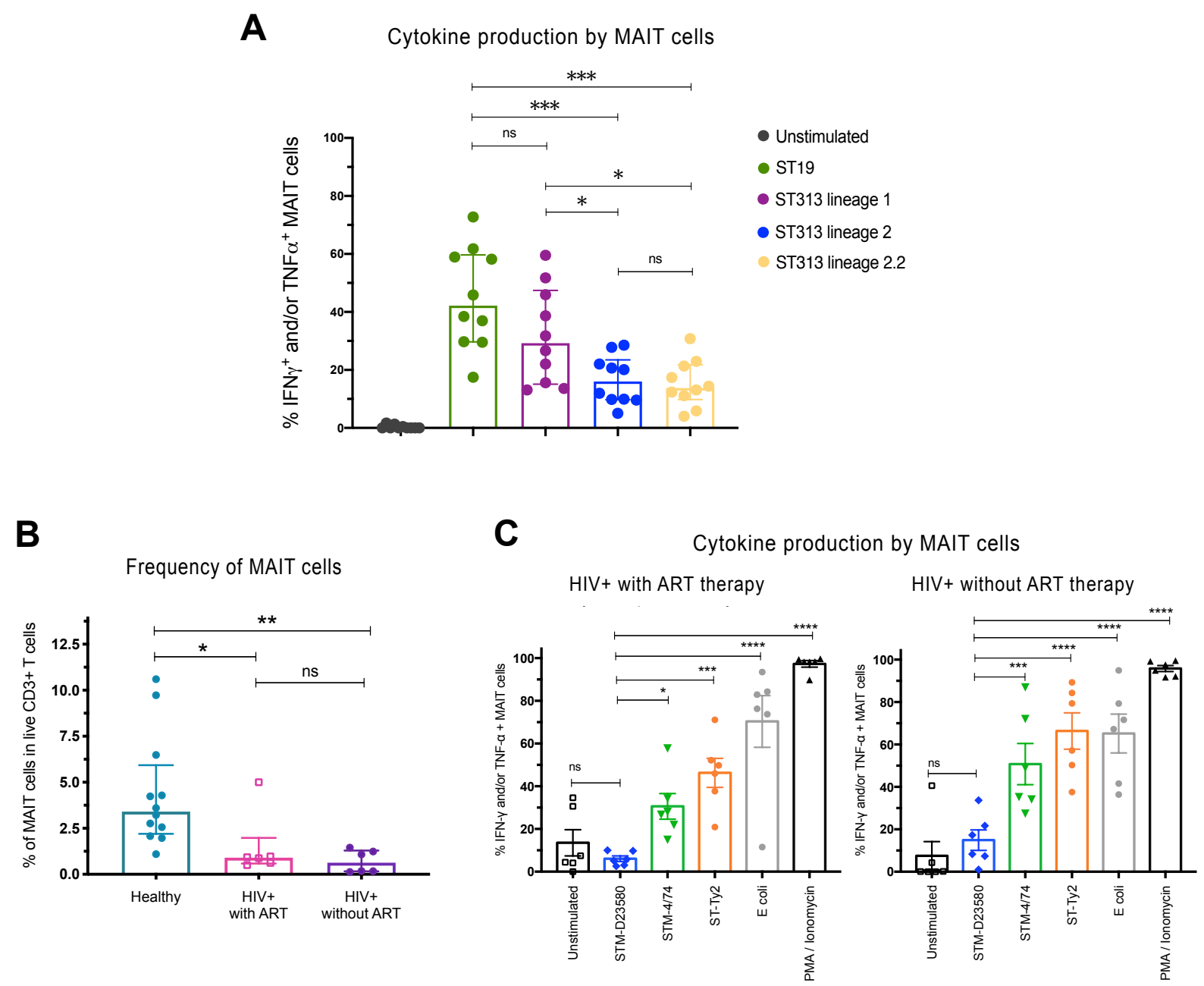
A
Cytokine production by MAIT cells
% IFNγ+ and/or TNFα+ MAIT cells
Unstimulated
ST19
ST313 lineage 1
ST313 lineage 2
ST313 lineage 2.2
B
Frequency of MAIT cells
% of MAIT cells in live CD3+ T cells
Healthy
HIV+ with ART
HIV+ without ART
C
Cytokine production by MAIT cells
HIV+ with ART therapy
HIV+ without ART therapy
% IFN-γ and/or TNF-α + MAIT cells
Unstimulated
STM-D23580
STM-4/74
ST-Ty2
E coli
PMA / Ionomycin

Figure 3

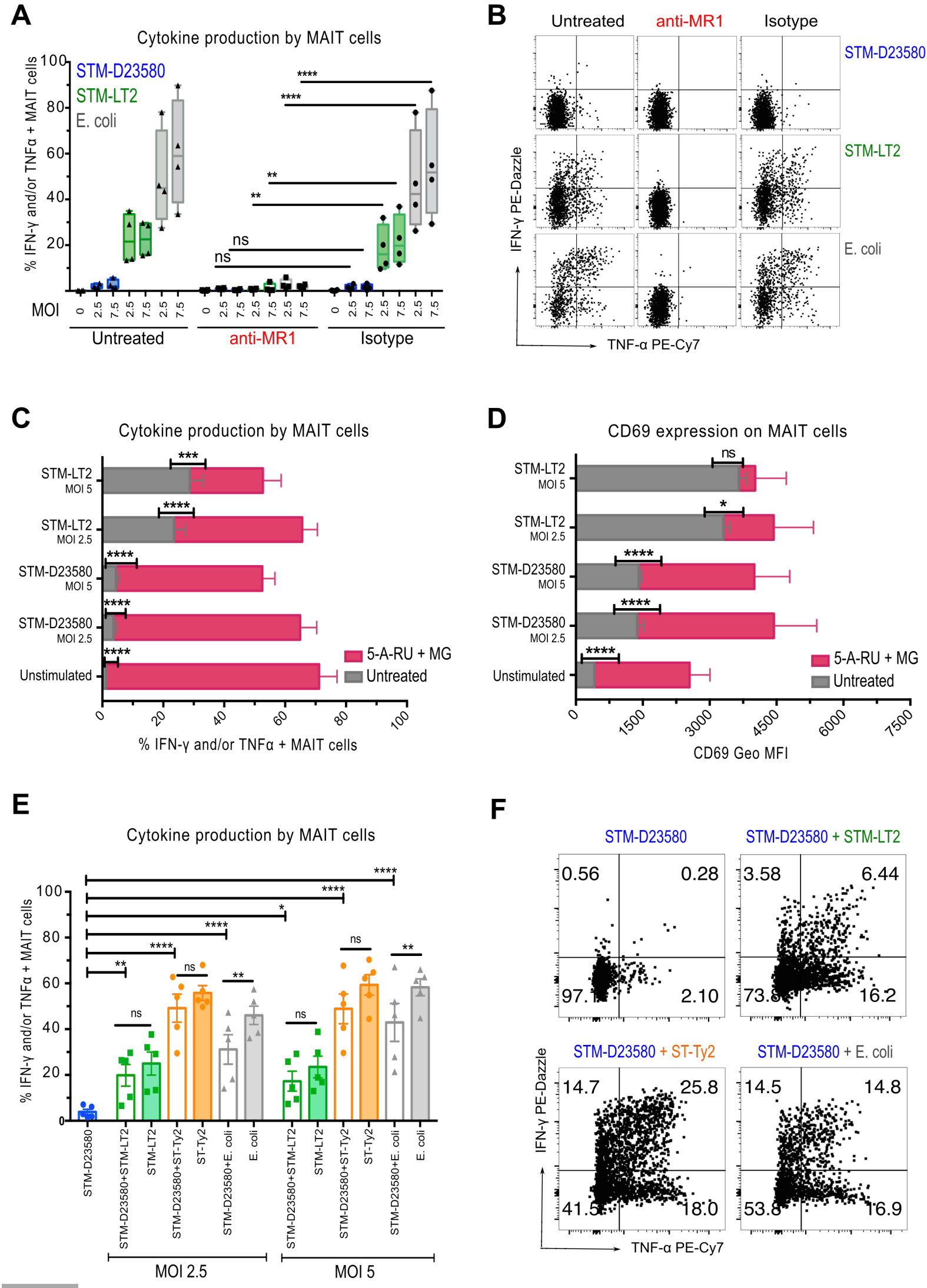
A
Cytokine production by MAIT cells
% IFN-γ and/or TNFα + MAIT cells
STM-D23580
STM-LT2
E. coli
MOI
Untreated
anti-MR1
Isotype
B
Untreated
anti-MR1
Isotype
STM-D23580
STM-LT2
E. coli
IFN-γ PE-Dazzle
TNF-α PE-Cy7
C
Cytokine production by MAIT cells
STM-LT2 MOI 5
STM-LT2 MOI 2.5
STM-D23580 MOI 5
STM-D23580 MOI 2.5
Unstimulated
5-A-RU + MG
Untreated
% IFN-γ and/or TNFα + MAIT cells
D
CD69 expression on MAIT cells
STM-LT2 MOI 5
STM-LT2 MOI 2.5
STM-D23580 MOI 5
STM-D23580 MOI 2.5
Unstimulated
5-A-RU + MG
Untreated
CD69 Geo MFI
E
Cytokine production by MAIT cells
% IFN-γ and/or TNFα + MAIT cells
STM-D23580
STM-D23580+STM-LT2
STM-LT2
STM-D23580+ST-Ty2
ST-Ty2
STM-D23580+E. coli
E. coli
MOI 2.5
MOI 5
F
STM-D23580
STM-D23580 + STM-LT2
0.56
0.28
97.
2.10
3.58
6.44
73.8
16.2
STM-D23580 + ST-Ty2
STM-D23580 + E. coli
14.7
25.8
41.5
18.0
14.5
14.8
53.8
16.9
IFN-γ PE-Dazzle
TNF-α PE-Cy7

Figure 4

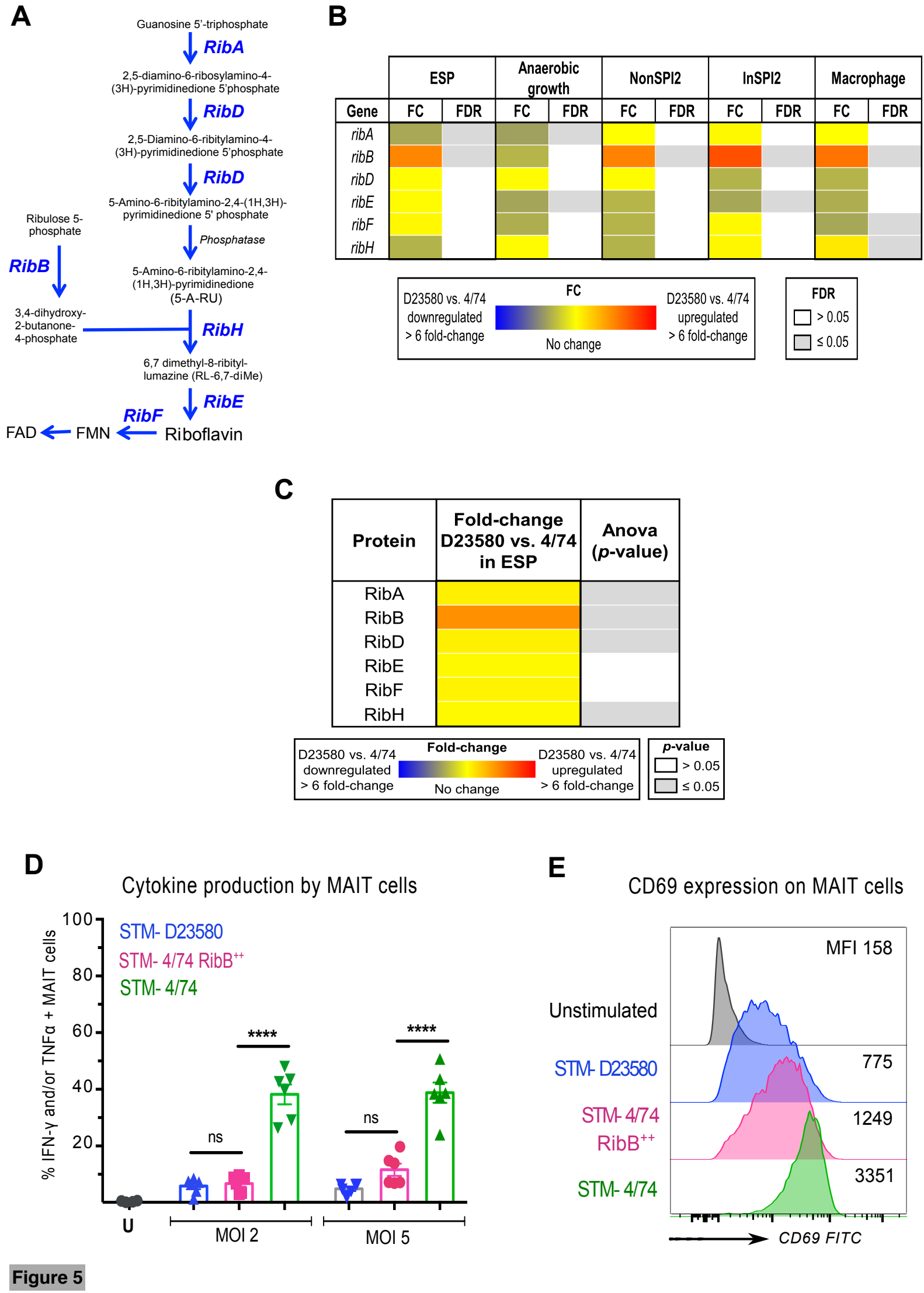
A
Guanosine 5'-triphosphate
RibA
2,5-diamino-6-ribosylamino-4-(3H)-pyrimidinedione 5'phosphate
RibD
2,5-Diamino-6-ribitylamino-4-(3H)-pyrimidinedione 5'phosphate
RibD
5-Amino-6-ribitylamino-2,4-(1H,3H)-pyrimidinedione 5' phosphate
Phosphatase
Ribulose 5-phosphate
RibB
5-Amino-6-ribitylamino-2,4-(1H,3H)-pyrimidinedione (5-A-RU)
3,4-dihydroxy-2-butanone-4-phosphate
RibH
6,7 dimethyl-8-ribityl-lumazine (RL-6,7-diMe)
RibE
RibF
FAD
FMN
Riboflavin
B
ESP
Anaerobic growth
NonSPI2
InSPI2
Macrophage
Gene
FC
FDR
ribA
ribB
ribD
ribE
ribF
ribH
D23580 vs. 4/74 downregulated > 6 fold-change
FC
No change
D23580 vs. 4/74 upregulated > 6 fold-change
FDR
> 0.05
≤ 0.05
C
Protein
Fold-change D23580 vs. 4/74 in ESP
Anova (p-value)
RibA
RibB
RibD
RibE
RibF
RibH
D23580 vs. 4/74 downregulated > 6 fold-change
Fold-change
No change
D23580 vs. 4/74 upregulated > 6 fold-change
p-value
> 0.05
≤ 0.05
D
Cytokine production by MAIT cells
% IFN-γ and/or TNFα + MAIT cells
100
80
60
40
20
STM- D23580
STM- 4/74 RibB++
STM- 4/74
****
****
ns
ns
U
MOI 2
MOI 5
E
CD69 expression on MAIT cells
Unstimulated
STM- D23580
STM- 4/74 RibB++
STM- 4/74
MFI 158
775
1249
3351
CD69 FITC

Figure 5

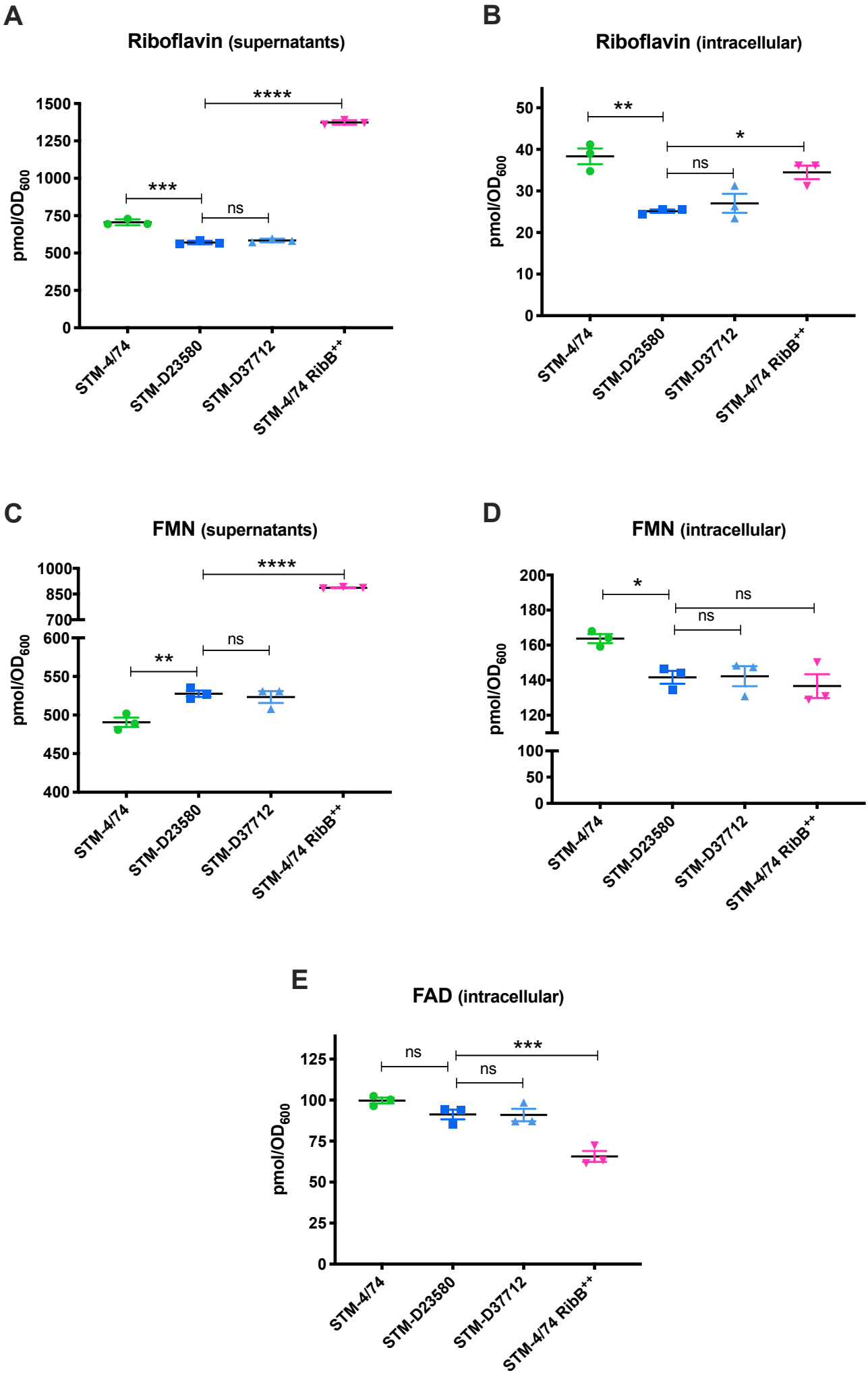
A
Riboflavin (supernatants)
pmol/OD600
1500
1250
1000
750
500
250
0
****
***
ns
STM-4/74
STM-D23580
STM-D37712
STM-4/74 RibB++
B
Riboflavin (intracellular)
pmol/OD600
50
40
30
20
10
0
**
*
ns
STM-4/74
STM-D23580
STM-D37712
STM-4/74 RibB++
C
FMN (supernatants)
pmol/OD600
1000
850
700
600
550
500
450
400
****
**
ns
STM-4/74
STM-D23580
STM-D37712
STM-4/74 RibB++
D
FMN (intracellular)
pmol/OD600
200
180
160
140
120
100
50
0
*
ns
ns
STM-4/74
STM-D23580
STM-D37712
STM-4/74 RibB++
E
FAD (intracellular)
pmol/OD600
125
100
75
50
25
0
ns
***
ns
STM-4/74
STM-D23580
STM-D37712
STM-4/74 RibB++

Figure 6